



Université du Québec
à Rimouski

**CONTRIBUTION À L'ÉTUDE DES PROPRIÉTÉS
OPTIQUES DES PARTICULES NON ALGALES
ORGANIQUES**

Mémoire présenté
dans le cadre du programme de maîtrise en océanographie
en vue de l'obtention du grade de maître ès sciences

PAR

© HABIBA BOUAKBA

Mars 2018

Composition du jury :

Huixiang Xie, président du jury, ISMER-UAQR

Martin Alejandro Montes, directeur de recherche, ISMER-UQAR

Jean-Pierre Gagné, codirecteur de recherche, ISMER-UQAR

Karem Chokmani, examinateur externe, INRS

Dépôt initial le 27 avril 2017

Dépôt final le 21 mars 2018

UNIVERSITÉ DU QUÉBEC À RIMOUSKI
Service de la bibliothèque

Avertissement

La diffusion de ce mémoire ou de cette thèse se fait dans le respect des droits de son auteur, qui a signé le formulaire «*Autorisation de reproduire et de diffuser un rapport, un mémoire ou une thèse*». En signant ce formulaire, l'auteur concède à l'Université du Québec à Rimouski une licence non exclusive d'utilisation et de publication de la totalité ou d'une partie importante de son travail de recherche pour des fins pédagogiques et non commerciales. Plus précisément, l'auteur autorise l'Université du Québec à Rimouski à reproduire, diffuser, prêter, distribuer ou vendre des copies de son travail de recherche à des fins non commerciales sur quelque support que ce soit, y compris l'Internet. Cette licence et cette autorisation n'entraînent pas une renonciation de la part de l'auteur à ses droits moraux ni à ses droits de propriété intellectuelle. Sauf entente contraire, l'auteur conserve la liberté de diffuser et de commercialiser ou non ce travail dont il possède un exemplaire.

'À mon Père et à ma Mère'

REMERCIEMENTS

Quels que soient les obstacles, la persévérance ainsi l'appui et la confiance des autres nous permettent d'avancer et d'atteindre nos objectifs. Ce travail de recherche n'aurait pu être complété tel qu'il a été espéré sans la supervision et les encouragements de mes deux directeurs de recherche, le professeur Martin Montes et le professeur Jean-Pierre Gagné, à qui je dois ma réussite.

Je remercie M. Montes pour son encadrement, ses commentaires pertinents, et son accompagnement qui ont fait de ce projet une expérience plus qu'enrichissante.

Je remercie sincèrement M. Jean-Pierre Gagné pour sa confiance, son écoute, sa patience, ses conseils et son optimisme qui m'ont donné la force de persévirer.

Un grand merci aux professeurs Huixiang Xie et Karem Chokmani d'avoir accepté d'évaluer mon mémoire et pour les multiples et précieuses corrections et suggestions.

Je remercie énormément Mme Karine Lemarchand pour son soutien qui m'a donné la force d'avancer, et Mme Martine Belzile pour sa gentillesse, son aide, sa générosité et son sourire qui me réconfortaient.

Je remercie tout particulièrement M. Hamou Sadat, professeur chercheur à l'université de Poitiers et ami de mon défunt père, pour son écoute et sa générosité.

Merci Saber Tlijani d'avoir été à mes côtés durant les moments difficiles, et de m'avoir motivée, épaulée et encouragée.

Je remercie vivement les professeurs Michel Gosselin, Emilien Pelletier et Gustavo Ferreira de m'avoir offert l'opportunité d'effectuer mes analyses et mes expériences dans leurs laboratoires respectifs.

Je voudrais également remercier Messieurs Adriano Magesky, Gholamreza Mohammadpour et Mathieu Millour , ainsi que l'ensemble des techniciens et agents de recherche de l'ISMER qui m'ont orientée, sans oublier mes amis et tous ceux qui m'ont apporté leur réconfort tout au long de ce projet.

Ce projet n'aurait pu voir le jour sans le financement offert par le Conseil de recherche en sciences naturelles et en génie (CRSNG) du Canada, que je remercie infiniment.

Finalement, TOUTE ma reconnaissance va vers mes parents, ma sœur et mon frère, qui n'ont eu cesse de croire en moi, de me soutenir et de m'encourager.

RÉSUMÉ

Les particules non-algales organiques (ONAP) représentent une grande partie des particules en suspension dans les milieux marins. Elles jouent un rôle important dans la chaîne alimentaire au sein de l'écosystème marin et font partie des constituants optiques.

L'objectif de cette étude est de caractériser les propriétés optiques inhérentes (IOPs) des ONAP à partir de mesures en laboratoire et de simulations effectuées avec des données biogéo-optiques *in situ*, obtenues dans l'Estuaire du St-Laurent (ESL). Les expériences en laboratoire comprenaient des mesures optiques de phytodétritus dérivés de deux espèces de phytoplancton, *Thalassiosira pseudonana* (TP) et *Dunaliella tertiolecta* (DT). Les coefficients d'absorption et de diffusion des ONAP (a_{ONAP} et b_{ONAP} , respectivement) ont été mesurés dans la gamme spectrale visible-proche-infrarouge (longueur d'onde = 412-715 nm), en utilisant un instrument de mesure d'absorption-atténuation (ac-9, WetLabs). Les coefficients optiques spécifiques à la masse (a_{ONAP}^* et b_{ONAP}^*) ont été calculés en normalisant les valeurs de a_{ONAP} et de b_{ONAP} par la concentration des ONAP par unité de volume. Un modèle d'estimation de a_{ONAP} et de b_{ONAP} dans les eaux de surface (ie, 0-5 m de profondeur) de l'ESL a été développé avec des déterminations *in situ* effectuées durant deux campagnes (mai 2000 et avril 2001) et des paramètres biogé-optiques rapportés dans la littérature.

Les résultats de laboratoire suggèrent des variations des IOPs des phytodétritus liées à des différences taxonomiques entre espèces de phytoplancton. En général, les détritus dérivés de DT avaient des valeurs de a_{ONAP}^* plus élevées en comparaison aux ONAP provenant des cellules de TP. Cette variation a été attribuée à la faible densité des phytodétritus dérivés des flagellés. De même, les valeurs élevées des ratios spectraux bleu / rouge de b_{ONAP}^* des phytodétritus des diatomées étaient liées à la présence d'opale.

Les estimations de a_{ONAP} par région et calculées pour l'ESL n'ont pas montré de changements importants entre les années. De plus, des ratios spectraux bleu/rouge de b_{ONAP} plus élevés ont été observées en mai 2000 par rapport aux calculs pour avril 2001. Cette variation était liée aux changements de la composition des ONAP entre les missions en raison de variations des espèces dominant de phytoplancton (ex. diatomées et des microflagellés en mai 2000 et en avril 2001, respectivement).

Mots clés : Propriétés optiques inhérentes, section transversale optique, particules non algales organiques, phytoplancton, détritus, bactérie, indice de réfraction.

ABSTRACT

Organic non-algal particles (ONAP) account for a large proportion of suspended particles in aquatic environments. They play an important role in the food chain within the marine ecosystem and represent a major optical component in littoral waters.

The objective of this study is to characterize the inherent optical properties (IOPs) of ONAP based on lab measurements and simulations performed with in situ biogeo-optical data obtained in the St Lawrence Estuary (SLE). Lab experiments encompassed bench optical measurements of phytodétritus derived from two phytoplankton species, *Thalassiosira pseudonana* (TP) and *Dunaliella tertiolecta* (DT). Absorption and scattering coefficients of ONAP (hereafter a_{ONAP} and b_{ONAP} , respectively) were measured within the visible-near-infrared spectral range (wavelength = 412-715 nm) using an absorption-attenuation meter (ac-9, WetLabs). Mass-specific optical coefficients (a_{ONAP}^* and b_{ONAP}^*) were computed by normalizing a_{ONAP} and b_{ONAP} values, respectively, by the concentration of ONAP per unit of volume. The model for estimating a_{ONAP} and b_{ONAP} in surface waters (i.e., 0-5 m depth) of the SLE was developed with in situ determinations made during two cruises (May 2000 and April 2001) and biogeo-optical parameters reported in the literature.

Lab results suggest optical changes on phytodetritus due to phytoplankton taxonomic differences. In general, DT-derived detritus tended to have higher a_{ONAP}^* values with respect to ONAP originated from TP cells. This variation was attributed to the lower apparent density of phytodetritus derived from microflagellates. Likewise, the larger blue/red spectral ratios of b_{ONAP}^* in phytodetritus samples of diatoms were linked to the presence of opal. Regionally-weighted a_{ONAP} estimates did not show substantial changes between years. Also, blue/red spectral ratios of b_{ONAP} were larger in May 2000 with respect to April 2001. This variation was related to changes on ONAP composition between surveys due different phytoplankton assemblages (e.g., dominance of diatoms and microflagellates during May 2000 and April 2001, respectively).

Keywords: Inherent optical properties, optical cross-section, organic non-algal particles, phytoplankton, detritus bacteria, refractive index.

TABLE DES MATIÈRES

REMERCIEMENTS	ix
RÉSUMÉ	xii
ABSTRACT	xiv
TABLE DES MATIÈRES.....	xv
LISTE DES TABLEAUX	xvii
LISTE DES FIGURES	xviii
LISTE DES ABRÉVIATIONS, DES SIGLES ET DES ACRONYMES	xxi
LISTE DES SYMBOLES	xxii
INTRODUCTION GÉNÉRALE	1
I. LA TÉLÉDÉTECTION OPTIQUE : CONCEPTS DE BASE.....	1
1.1 INTERACTION DE LA LUMIERE AVEC L'ATMOSPHERE ET LE MILIEU MARIN.....	2
1.2 CONSTITUANTS BIOGEO-OPTIQUES DE L'OCEAN.....	4
II. L'ESTUAIRE DU SAINT-LAURENT	8
III. OBJECTIFS DU MÉMOIRE	9
CHAPITRE 1. PROPRIÉTÉS OPTIQUES DES PARTICULES NON ALGALES ORGANIQUES ISSUES DE CULTURE DE PHYTOPLANCTON ET DE MESURES IN SITU.....	11
1.1 RESUME EN FRANÇAIS DU PREMIER ARTICLE	11
1.2 ABSTRACT	13
1.3 INTRODUCTION	14
1.4 MATERIALS AND METHODS	21

1.4.1. LAB MEASUREMENTS	21
1.4.2. <i>In situ</i> datasets.....	26
1.5 RESULTS	31
1.5.1. Lab measurements	31
1.5.2. Size distribution of phytodetritus.....	36
1.5.3. Field measurements	37
1.6 DISCUSSION.....	39
1.6.1. Lab-derived optical properties of phytodetritus.....	41
1.6.2. Uncertainties of modeled ONAP coefficients for the SLE.....	43
1.6.3. Optical properties of ONAP in the SLE	45
1.7 CONCLUSIONS	49
CONCLUSION GÉNÉRALE	52
RÉFÉRENCES BIBLIOGRAPHIQUES	56

LISTE DES TABLEAUX

Tableau 1 : Différentes propriétés optiques utilisées en optique hydrologique selon..... 3

Chapitre 1

Tableau 1 : List of acronyms 15

Tableau 2 : Modeled mass-specific absorption and scattering coefficients of ONAP
based on *in situ* measurements. Between parentheses are ± 2 standard errors..... 39

LISTE DES FIGURES

Figure 1 : Variation du coefficient d'absorption de l'eau pure. Représentation graphique des données obtenues dans Pope et Fry (1997)	5
Figure 2 : Spectres d'absorption de la lumière par différents pigments photosynthétiques et photoprotecteurs dilués dans de l'acétone à 90% ; chl <i>a</i> , chlorophylle <i>a</i> ; chl <i>b</i> , chlorophylle <i>b</i> ; chl <i>c</i> , chlorophylle <i>c</i> ; Bchl <i>a</i> , bactériochlorophylle <i>a</i> ; b-car, β carotène, et des formes naturelles de phycobiline (phyc) extraite à partir d'algue (Wozniak and Ostrowska, 1991).	6

Chapitre 1

Figure 1 : Sampling locations during May 2000 (green circles) and April 2001 (orange rectangles) cruises. The main tributary of the St. Lawrence Estuary (i.e., Saguenay River) is indicated.....	27
Figure 2 : Phytoplankton cell disruption due to thermal and acoustic stress. Chlorophyll <i>a</i> concentration in DT (blue symbols) and TP (red symbols) samples collected during the senescent phase of phytoplankton growth curve and treated at different time lags. Uncertainty bars indicate ± 2 standard errors.....	32
Figure 3 : Optical contribution of heterotrophic bacteria to spectral absorption and scattering coefficients of phytodetritus. a) bacterial absorption, and b) bacterial scattering. DT (blue symbols) and TP (red symbols).....	33
Figure 4 : Spectrally-normalized optical coefficients of phytodetritus. a) particulate absorption, and b) particulate scattering; DT (blue symbols) and TP (red symbols)	34
Figure 5 : Mass-specific absorption and scattering coefficients of phytodetritus. a) particulate absorption, and b) particulate scattering; DT (blue symbols) and TP(red symbols).	35
Figure 6 : Particle size distribution of phytodetritus. Log-transformed number of detrital particles (Ndet) for different size bins (x-axis). DT- (solid black) and TP-derived detritus (solid grey).....	37

Figure 7 : Modeled spectral absorption and scattering coefficients of ONAP in the SLE. a) particulate absorption, and b) particulate scattering; May 2000 (empty circles), April 2001 (solid circles). Negative values of b_{ONAP} are not shown 38

LISTE DES ABRÉVIATIONS, DES SIGLES ET DES ACRONYMES

ESL	Saint Lawrence Estuary
IOPs	Inherent Optical Properties
AOPs	Apparent Optical Properties
NAP	Non-algal Particles
ONAP	Organic non algal particules
INAP	Inorganic non-algal particulates
CDOM	Chromophoric dissolved organic matter
chl	Chlorophyll a concentration
POM	Particulate organic patter
PIM	Particulate inorganic matter
POC	Particulate organic carbon
PSD	Particulate size distribution

LISTE DES SYMBOLES

Chl	chlorophyll a concentration
chl/C	chlorophyll a-to-particulate Carbon ratio
[PIM]	particulate inorganic matter concentration
[POM]	particulate organic matter concentration
[POM^{phyto}]	concentration of POM associated to phytoplankton
[POM^{ONAP}]	concentration of POM associated to ONAP
[POC^{phyto}]	concentration particulate organic carbon associated to phytoplankton
f1	$[POC^{phyto}]/[chl]$ ratio
f2	$[POM^{phyto}]/[POC^{phyto}]$ ratio
λ	Wavelength
A	total absorption coefficient
a_w	absorption coefficient of pure seawater
a_p	absorption coefficient of particulates
a_{ph}	absorption coefficient of phytoplankton
a_{nw}	absorption coefficient of phytodetritus suspensions
a_{CDOM}	absorption coefficient of chromophoric dissolved organic matter

a_{NAP}	absorption coefficient of NAP
a_{NAP}^*	mass-specific absorption coefficient of NAP
a_{ONAP}	absorption coefficient of ONAP
a_{ONAP}^*	mass-specific absorption coefficient of ONAP
a_{POM}	absorption coefficient of POM
a_{POM}^*	mass-specific absorption coefficient of POM
a_{PIM}	absorption coefficient of PIM
a_{PIM}^*	mass-specific absorption coefficient of PIM
a_p^*	mass-specific absorption coefficient of particulates
a_{ph}^*	mass-specific absorption coefficient of phytoplankton
a_{diss}	absorption coefficient of dissolved matter after filtering through 0.7 μm membranes
b_{diss}	scattering coefficient of dissolved matter after filtering through 0.7 μm membranes
c_{diss}	beam attenuation coefficient of dissolved matter after filtering through 0.7 μm membranes
c_{nw}	beam attenuation coefficient of phytodetritus suspensions
c_p	beam attenuation coefficient of particulates
c_{ph}	beam attenuation coefficient of phytoplankton

b_p^*	mass-specific scattering coefficient of particulates
B	total scattering coefficient
b_w	scattering coefficient of pure seawater
b_{nw}	scattering coefficient of phytodetritus suspensions
b_p	scattering coefficient of particulates
b_{ph}	scattering coefficient of phytoplankton
b_{ONAP}	scattering coefficient of ONAP
b_{ONAP}^*	mass-specific scattering coefficient of ONAP
c_{ONAP}	beam attenuation coefficient of ONAP
b_{POM}	scattering coefficient of POM
b_{PIM}	scattering coefficient of PIM
σ_c^{bact}	attenuation cross section of heterotrophic bacteria
σ_a^{HB}	absorption cross section of heterotrophic bacteria
σ_b^{HB}	scattering cross section of heterotrophic bacteria
N_{HB}	number of heterotrophic bacteria
a_{HB}	absorption coefficient of heterotrophic bacteria
b_{HB}	scattering coefficient of heterotrophic bacteria
c_{HB}	beam attenuation coefficient of heterotrophic bacteria

VSF Volume scattering function

INTRODUCTION GÉNÉRALE

Durant les deux dernières décennies, la télédétection de la couleur de l'océan a connu un développement important grâce aux avancées technologiques dans le domaine spatial. Cet outil offre la possibilité d'effectuer des études portant sur les différents processus, physiques, chimiques, biologiques et géologiques qui régissent le milieu marin. Elle permet, par exemple, de mieux comprendre les variations spatio-temporelles de la distribution du carbone organique, de la productivité primaire, ainsi que d'estimer la température de la surface de l'océan (Platt et al., 1989) .

Un grand nombre d'algorithmes a été développé dans le but de caractériser les propriétés optiques et biogéo-chimiques des milieux marins (Morel et al., 1989; Mobley, 1999). Ces modèles varient constamment en raison des nouvelles informations obtenues grâce, d'une part, aux données optiques collectées *in situ* mais aussi, à l'augmentation de la résolution spectrale et spatiale des instruments de mesures. Afin de valider ces différents modèles, il est nécessaire de comprendre comment la lumière interagit avec les composantes biogéo-optiques du milieu marin (Reynolds et al, 2001).

I. LA TÉLÉDÉTECTION OPTIQUE : CONCEPTS DE BASE

La télédétection optique permet d'étudier, à distance, l'interaction de la lumière avec un objet ciblé. En d'autres termes, elle permet d'analyser le comportement optique de l'objet, offrant ainsi des informations sur ses caractéristiques physiques et chimiques, sans contact direct. Elle concerne les spectres de l'UV (≤ 400 nm), du visible (de 400 à 700 nm) et du proche-moyen infrarouge (IR) (de 700 à 3000 nm). Le processus de collecte de données se fait grâce à une combinaison de différents éléments composant le système de télédétection. Ce dernier est constitué en général, d'une source de lumière, naturelle en cas de télédétection passive ou artificielle en cas de télédétection active, de la cible étudiée qui

interagit avec les spectres de lumière, d'un capteur ou senseur satellitaire, et du milieu optique regroupant les éléments précédents.

1.1 INTERACTION DE LA LUMIÈRE AVEC L'ATMOSPHÈRE ET LE MILIEU MARIN

Quand un rayon lumineux atteint la surface de la mer, après modification par les composantes atmosphériques, une partie de ce rayon est absorbée, et une autre partie transmise y est réfractée. En fonction de la longueur d'onde, l'eau et ses constituants absorbent et diffusent la partie de la lumière. Une fraction de cette lumière atteindra le fond dans le cas d'une turbidité relativement et d'une profondeur relativement faible. Si les photons rétrodiffusés font partie du champ de vision (FOV, Field Of View) d'un senseur aéroporté ou satellitaire, ils seront détectés par ce dernier après modifications qualitatives (changement spectral) et quantitatives (atténuation de l'énergie) dans l'atmosphère et la surface de la mer. Il faut savoir que les données collectées dépendent fortement de la couverture nuageuse et la distribution d'aérosols de la région d'étude. Le signal mesuré par le capteur satellitaire correspond à trois contributions différentes de la radiance par la surface de la mer, les eaux de surface de l'océan, et la diffusion atmosphérique. On peut distinguer deux types de propriétés optiques caractérisant les milieux océaniques: Les propriétés optiques apparentes (en anglais, Apparent Optical Properties ou AOPs) et les propriétés optiques inhérentes (en anglais, Inherent Optical Properties ou IOPs) (Preisendorfer, 1961). Les différentes AOPs et IOPs utilisées en optique hydrologique sont résumées dans le tableau 1. Les AOPs dépendent de la structure géométrique de la distribution de la radiance ou l'énergie par unité de surface et angle solide, et de la nature des composantes optiques.

La réflectance de télédétection, R_{rs} , à la longueur d'onde λ est le principal paramètre utilisé dans les algorithmes de la 'couleur de l'eau' (tableau 1). Cette réflectance est définie comme étant le rapport entre la luminance de l'eau $L_w(\lambda)$, à l'éclairement descendant $E_d(\lambda)$ juste au-dessus la surface de l'eau (symbole $^+$) (équation 1).

$$R_{rs}(\lambda)^+ = L_w(\lambda)^+ / E_d(\lambda)^+ \quad (1)$$

Contrairement aux AOPs, les IOPs dépendent uniquement de la nature (taille, forme, et composition chimique des particules) et de la concentration des composantes optiques dans le milieu (Mobley, 1994).

Tableau 1 : Différentes propriétés optiques utilisées en optique hydrologique selon Mobley (1994)

AOPs		
Quantité	Symbol	Unité
Luminance montante au-dessus la surface de l'eau	L_w	$\text{W m}^{-2} \text{ sr}^{-1} \text{ nm}^{-1}$
ÉCLAIREMENT DESCENDANT	E_d	$\text{W m}^{-2} \text{ nm}^{-1}$
RÉFLECTANCE DE TÉLÉDÉTECTION	R_{rs}	sr^{-1}
IOPs		
Coefficient d'atténuation de faisceaux	C	m^{-1}
Coefficient d'absorption	a	m^{-1}
Coefficient de diffusion	b	m^{-1}
Coefficient de rétrodiffusion	b_b	m^{-1}
Coefficient angulaire de diffusion	β	$\text{m}^{-1} \text{ sr}^{-1}$

Parmi les principales propriétés optiques inhérentes étudiées en milieu marin, on retrouve le coefficient d'atténuation, c . L'atténuation est définie pour une longueur d'onde spécifique comme étant la quantité d'énergie perdue à cause de l'absorption et de la diffusion des photons. L'absorption, représentée par le coefficient d'absorption, a , est la fraction absorbée par les composantes optiques. La diffusion, ayant comme, b , est le phénomène qui augmente l'atténuation des photons. Les coefficients, a , b , et c varient en fonction de la longueur d'onde du rayon lumineux incident.

$$c(\lambda) = a(\lambda) + b(\lambda) \quad (2)$$

Les équations décrivant les IOPs ci-dessous (Sathyendranath et Morel, 1983) montrent que ces propriétés dépendent de la contribution optique de l'eau (indice w), de la concentration de la matière organique dissoute colorée (indice CDOM), du phytoplancton (indice ph) et des détritus définis comme étant les particules non algales organiques et inorganiques (indice NAP) en notant que la contribution de CDOM à la diffusion, est négligeable. Tous ces constituants varient eux aussi en fonction de la longueur d'onde.

$$a(\lambda) = a_w(\lambda) + a_{ph}(\lambda) + a_{NAP}(\lambda) + a_{CDOM}(\lambda) \quad (3)$$

$$b(\lambda) = b_w(\lambda) + b_{ph}(\lambda) + b_{NAP}(\lambda) \quad (4)$$

$$b_b(\lambda) = b_{bw}(\lambda) + b_{bph}(\lambda) + b_{bNAP}(\lambda) \quad (5)$$

a , b , c et b_b représentent respectivement les coefficients d'absorption, de diffusion, d'atténuation et de rétrodiffusion de la lumière. Le coefficient de rétrodiffusion est défini comme étant la diffusion de photons en arrière et pour des angles entre $\pi/2$ et π . De ce fait, et tel que montré par l'équation 6, la réflectance peut également être exprimée en fonction du b_b et du a (Gordon *et al.*, 1975, Morel & Prieur, 1977, Gordon *et al.*, 1988).

$$R_{rs}(\lambda) = f/Q \cdot b_b(\lambda) / (a(\lambda) + b_b(\lambda)) \quad (6)$$

f/Q est une variable qui dépend de l'angle zénithal solaire, des propriétés optiques de l'eau de mer et de la longueur d'onde de la lumière (Morel et Gentili, 1991; Morel et Gentili, 1996). L'équation 6 confirme que les AOPs d'un milieu marin dépendent directement des IOPs de ce milieu et des constituants biogéo-optiques de l'océan.

1.2 CONSTITUANTS BIOGÉO-OPTIQUES DE L'OCÉAN

1.2.1 L'absorption de la lumière

L'eau de mer pure, constituée par l'eau pure et les minéraux dissous, absorbe la lumière de

manière importante dans le domaine spectral rouge (Figures 1 et 3). Cette absorption est influencée par la température et la salinité de l'eau (Pope et Fry, 1997, Röttgers et al. 2014) Les changements optiques au niveau de la composition moléculaire et la structure l'eau sont pas bien connues (Pope et Fry, 1997).

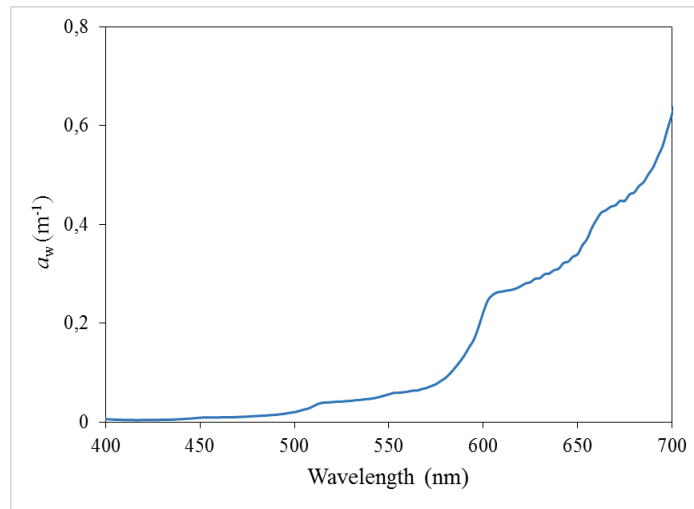


Figure 1 : Variation du coefficient d'absorption de l'eau pure. Représentation graphique des données obtenues dans Pope et Fry (1997).

L'absorption par les différentes espèces de phytoplancton rencontrées en milieu marin varie en fonction de leurs concentrations en pigments photosynthétiques et photoprotecteurs (Figure 2). La chlorophylle-*a* est le pigment le plus commun dans tous les groupes du phytoplancton. La molécule de chlorophylle-*a*, après extraction à l'acétone (concentration finale 90%), a une absorption maximale de la lumière principalement dans la région spectrale bleue (maximum centre à $\lambda = 440$ nm) et dans le rouge ($\lambda = 665$ nm) (Figure 2).

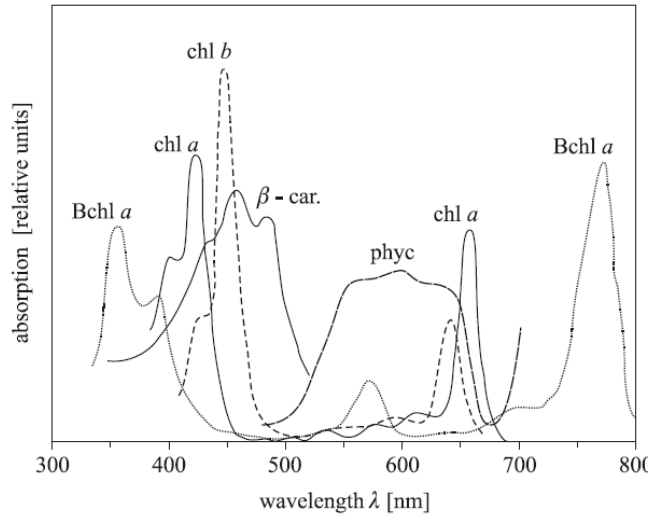


Figure 2 : Spectres d'absorption de la lumière par différents pigments photosynthétiques et photoprotecteurs dilués dans de l'acétone à 90% ; chl *a*, chlorophylle *a*; chl *b*, chlorophylle *b*; chl *c*, chlorophylle *c*; Bchl *a*, bactériochlorophylle *a*; b-car, β carotène, et des formes naturelles de phycobiline (phyc) extraite à partir d'algue (Wozniak and Ostrowska, 1991).

L'eau de mer contient des concentrations variables de matière organique dissous colorée (CDOM). Elle est définie comme étant la fraction de la matière organique colorée ayant une taille inférieure à $0.2 \mu\text{m}$ (Vodacek et al., 1995) et qui est constituée en grande partie d'acides humiques et fluviques (Carder et al. 1989 ,Vodacek 1992, Vodacek et al. 1997).

L'absorption de la lumière par CDOM est plus importante dans le spectre bleu et diminue de façon exponentielle dans les plus grandes longueurs d'ondes présente une diminution de façon exponentielle dans le spectre rouge (Figure 3). En outre, le coefficient d'absorption de CDOM fournit des informations utiles sur les processus biogéochimiques (Carder et al., 1989, Nelson et al., 2007), l'activité microbienne en milieu marin (Nelson et al., 1998) et les processus photochimiques (Xie et al., 2009).

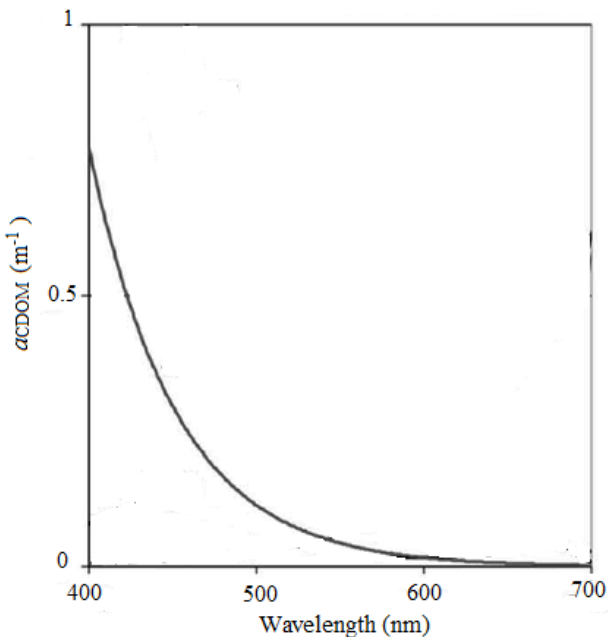


Figure 3 : Variation du coefficient d'absorption de CDOM en eau de mer (figure modifiée de Turpie, 2013).

Les particules non algales, ou NAP, regroupent les particules non algales d'origine inorganique (INAP) et organique (ONAP). Les INAP sont créées principalement par l'altération des roches terrestres et des sols. Ces particules peuvent pénétrer dans l'eau à mesure que la poussière terrestre emportée par le vent s'installe à la surface de la mer. Ils ont également comme origine l'exosquelette de certaines espèces de phytoplancton qui produisent la calcite (coccolithophores) ou de la silice (frustules de diatomées). Ces dernières sont présentes au niveau des fonds sous-marins sous forme de particules et sont remises en suspension grâce aux courants marins.

Le composantes ONAP sont incluent les particules organiques non vivantes, appelées aussi détritus organiques. Les détritus organiques peuvent être représentées par les cellules phytoplanctoniques mortes, les produits organiques issus de la dégradation de la matière organique par des bactéries, ou peuvent résulter du broutage du phytoplancton par le

zooplancton sous formes de fragments de cellules et de pelotes fécales (Stukel et al., 2014). Finalement, les ONAP englobent les bactéries, les champignons, des virus et le zooplancton mort.

Quelques études se sont attachées à définir les propriétés optiques de certaines ONAP composants en milieu marin. Le comportement optique des bactéries hétérotrophiques marines a été rapporté dans Stramski et Kiefer (1990) confirmant ainsi le rôle que jouent les ONAP dans l'absorption et la diffusion de la lumière en milieu océanique. Cependant, très peu d'études se sont intéressées à l'analyse des IOPs des phytodétritus marins (ides détritus dérivés des cellules phytoplanctoniques) (Nelson, 1993). Des détritus organiques jouent un rôle important dans le cycle biogéochimique en milieu marin. L'importance d'un type particulier de détritus organiques dans un écosystème dépend d'un certain nombre de caractéristiques comme sa taille et sa nature chimique (Smith, 2006). Les phytodétritus peuvent garder une partie des pigments photosynthétiques au moment de leur production. Cependant, cette partie est vite dégradée, et par conséquent, l'absorption de la lumière par ces particules est très importante dans le domaine spectral du bleu, en comparaison avec les autres domaines spectraux (Mobley, 2010). Les modèles biogéo-optiques actuels n'offrent pas la possibilité de discriminer les IOPs des ONAP de celles des INAP.

II. L'ESTUAIRE DU SAINT-LAURENT

Du point de vue optique, les milieux marins peuvent être partagés en deux catégories. Des eaux dites de Cas 1 et des eaux appartenant au Cas 2 (Morel et Prieur, 1977). Les eaux du Cas 1 représentent les milieux marins qui ne sont pas influencés par les apports terrigènes. Les eaux du Cas 2 quant à elles, sont beaucoup plus complexes que les eaux du Cas 1 en raison de la diversité des constituants qui leur sont associés comme des composantes additionnelles dérivées des rivières (sédiments des rivières) (Carder et al. 1989). Par conséquent, les eaux des estuaires peuvent être considérées comme des eaux du Cas 2. Ces

définitions ont été contestées à travers différentes études (Maritorena et al., 2004 ; Mobley et al., 2004) car des eaux optiquement complexes peuvent se former dans l'océan (cas d'un bloom phytoplanctonique ou d'un bloom de coccolithophores) (Mobley, 2004).

L'estuaire du Saint-Laurent (ESL), situé au niveau de la région du Québec, au Canada, représente une excellente zone pour l'étude des propriétés optiques des ONAP car il combine les caractéristiques des eaux du Cas 2 (eaux du fleuve Saint-Laurent) et du Cas 1 (eaux du Golfe du Saint-Laurent) (Babin et al., 1993). La composition optique des eaux de l'ESL est caractérisée par les différentes contributions dérivées de la grande variété de matière organique dissoute et particulaire en suspension, due aux différentes sources terrigènes et océaniques (El-Sabh et Silverberg, 1992).

Du point de vue optique, l'ESL reste encore peu étudié. Toutefois, quelques études (Babin 1993, Larouche et Boyer-Villemaire 2010, Montes-Hugo et al. 2012) se sont intéressées à ses caractéristiques optiques et à leur influence sur la couleur de l'océan. De plus, des études telles que celles de Larouche and Boyer-Villemaire, (2010) et celles de Xie et al. (2012) ont apporté de nouvelles informations traitant des IOPs des NAP présentes au niveau de l'ESL. Cependant, les IOPs des ONAP au niveau de l'ESL sont, à ce jour, inconnues.

III OBJECTIFS DU MÉMOIRE

Contrairement aux autres composantes, les particules non algales organiques ont été très peu étudiées et leurs propriétés optiques ainsi que l'importance de leur contribution à la variation du signal satellitaire restent mal connues. De plus; les algorithmes de télédétection actuels ne permettent pas d'estimer les IOPs des ONAP et définir leur impact dans les IOPs. Pour les eaux de l'estuaire du St-Laurent (ESL), les principaux objectifs de ce projet sont :

- De caractériser les propriétés optiques des phytodétritus dérivées de deux espèces de phytoplancton (*Thalassiosira pseudonana* et *Dunaliella tertiolecta*) par des mesures en laboratoire.
- De modéliser les propriétés optiques des phytodétritus issus de données collectées *in situ*, au niveau de l'ESL.
- D'étudier l'influence des variables environnementales telles que les apports fluviaux, sur la distribution des ONAP modélisées dans l'ESL.

CHAPITRE 1

PROPRIETES OPTIQUES DES PARTICULES NON ALGALES ORGANIQUES ISSUES DE CULTURE DE PHYTOPLANCTON ET DE MESURES IN SITU

1.1 RÉSUMÉ EN FRANÇAIS DU PREMIER ARTICLE

Les coefficients optiques de particules organiques non algales (ONAP) ont été déterminés en laboratoire à partir de mesures sur des phytodétritus issus de cultures phytoplanctoniques de *Thalassiosira pseudonana* (TP) et de *Dunaliella tertiolecta* (DT) et de simulations par des mesures optiques *in situ* effectuées dans des eaux de surface (0-2 m de profondeur) de l'estuaire du Saint-Laurent (SLE), en mai 2000 et avril 2001. Des particules de phytodétritus ont été produites artificiellement en exposant des cellules en phase de croissance sénesciente à de multiples cycles de décongélation / congélation et à une sonification. Des déterminations optiques d'absorption (a_{ONAP}) et de diffusion (b_{ONAP}) de phytodétritus ont été obtenues dans la gamme spectrale visible-proche-infrarouge ($\lambda = 412\text{-}715$ nm) avec un absorbeur-atténuateur-mètre (ac-9, WetLabs). Les variations des coefficients optiques dues à la manipulation des échantillons et à la contamination associée aux phytodétritus par des bactéries hétérotrophes ont été minimisées. L'incertitude sur les mesures a_{ONAP} et b_{ONAP} était importante (par exemple, at $\lambda = 443$ nm, jusqu'à 50% et 75%, respectivement), et rendait difficile la discrimination optique des particules détritiques dérivées de différentes espèces de phytoplancton. Cependant, les spectres de b_{ONAP} normalisés à $\lambda = 412$ nm ont semblé montrer que les phytodétritus de diatomées ont une diffusion plus grande dans la gamme bleue en raison de la présence de silice biogénique. Des estimations a_{ONAP} normalisées par le poids (a_{ONAP}^*) à une masse élevée (jusqu'à 0,11 $\text{m}^2 \text{ g}^{-1}$ à $\lambda = 440$ nm) ont été associées à des détritus dérivés de DT. Ce profil était en partie expliqué par la densité apparente relativement faible des cellules DT et des détritus dérivés de DT. Contrairement à a_{ONAP} , les valeurs de b_{ONAP} modélisées au printemps, au niveau du

ESL ont révélé des changements interannuels importants liés aux changements sur la diffusion totale des particules due aux minéraux. Enfin, les changements spectraux sur les moyennes régionales de b_{ONAP} coïncidaient avec de larges modifications des communautés phytoplanctoniques dominantes dans le SLE (par exemple, diatomées vs microflagellés).

Cet article, intitulé « *Optical properties of organic detritus derived from phytoplankton cultures and in situ measurements* », fut corédigé par moi-même ainsi que par le professeur Martin-Montes et révisé par le professeur Jean-Pierre Gagné. Il sera soumis sous peu pour publication, au journal Marine Ecology Progress Series (MEPS). En tant que premier auteur, ma contribution à ce travail fut l'essentiel de la recherche sur l'état de l'art, le développement de la méthode, l'exécution des tests de performance et la rédaction de l'article. Le professeur Martin Montes a fourni l'idée originale. Il a aidé à la recherche sur l'état de l'art, au développement de la méthode ainsi qu'à la révision de l'article. Le professeur Jean-Pierre Gagné a aidé au développement de la méthode ainsi qu'à la révision de l'article.

Optical properties of organic detritus derived from phytoplankton cultures and in situ measurements

Habiba Bouakba, Martin A. Montes-Hugo, Jean-Pierre Gagné

Institut des Sciences de la Mer de Rimouski, 310 Allée des Ursulines, Office P-216, Rimouski, Québec,
Canada, G5L 3A1

Correspondence to: Martin A. Montes-Hugo (martinalejandro_montes@uqar.ca)

1.2 ABSTRACT

Optical coefficients of organic non-algal particulates (ONAP) were determined based on lab measurements of phytodetritus derived from two phytoplankton cultures (*Thalassiosira pseudonana* and *Dunaliella tertiolecta*, TP and DT, respectively) and simulations constrained with *in situ* optical measurements made in surface waters (i.e., 0-2 m depth) of the St. Lawrence Estuary (SLE) during May 2000 and April 2001. Phytodetritus particles were artificially produced by exposing cells in the senescent growth phase to multiple thawing/freezing and sonication cycles. Lab optical determinations of absorption (a_{ONAP}) and scattering (b_{ONAP}) coefficients of phytodetritus were obtained within the visible-near-infrared spectral range (i.e., $\lambda = 412\text{-}715\text{ nm}$) with an absorption-attenuation-meter (ac-9, WetLabs). Changes on optical coefficients due to sample handling and associated contamination of phytodetritus by heterotrophic bacteria were minimized. The uncertainty on a_{ONAP} and b_{ONAP} measurements was large (e.g., at $\lambda = 412\text{ nm}$, up to 50% and 75%, respectively) and made difficult the optical discrimination of detrital particles derived from different phytoplankton species. However, spectrally-normalized b_{ONAP} spectra appeared to show that diatom phytodetritus have a preferential absorption in the blue range due likely to the presence of biogenic silica. High (up to $0.11\text{ m}^2\text{ g}^{-1}$ at $\lambda = 440\text{ nm}$) mass-specific a_{ONAP} (a_{ONAP}^*) estimates were associated to DT-derived detritus. This pattern was in part explained by the relatively low apparent density of DT cells and DT-derived detritus.

Unlike a_{ONAP} , modeled b_{ONAP} values in the SLE and during spring revealed important inter-annual changes connected with changes on total particulate scattering due to minerals. Lastly, spectral changes on regional means of b_{ONAP} coincided with wide modifications of dominant phytoplankton communities in the SLE (e.g., diatoms vs microflagellates).

1.3 INTRODUCTION

Coastal waters are known to be highly variable in terms of optical properties due to the contribution of particulates and dissolved colored substances having different origins (e.g., sediment, water column, land) (Green et al., 2003; Lee and Hu, 2006). A substantial fraction of this variability is attributed to changes associated to non-algal particulates (NAP). The organic fraction of NAP (ONAP) is mainly associated to non-living particulate material; however, it may include living organisms such as zooplankton, fungi, microheterotrophs (e.g., ciliates, flagellates) and particle-attached bacteria (Green et al., 2003; Dunne et al. 2005; Stukel et al., 2014).

Plankton is the principal source of ONAP in the ocean (Roman 1984; Melack, 1985; Nelson 1993; Boyd and Newton, 1995). Plankton-derived detritus are very diverse (e.g., fecal pellets, fragments of phytoplankton cells, zooplankton molting carcasses) (Stukel et al., 2014). Also, organic detritus in some marine environments may originate from floating macroalgae (e.g., Sargasso Sea) (Menzel, 1966) or even death bodies (e.g., whales) (Higgs et al., 2014). In littoral waters, ONAP composition is more complex due to the addition of organic debris derived from vascular plants (e.g., seagrass) (Thresher, 1992) and benthic macroalgae (Karlson, 2016). Lastly, ONAP may include particle aggregates having a mixed composition of inorganic and organic constituents (e.g., transparent exopolymeric particles) (Stavn, 2012; Annane et al., 2015).

Autochthonous production of ONAP is related to multiple processes (e.g., egestion of fecal pellets, viral lysis of bacteria, death of microbes, molting or death of zooplankton) (Stukel

et al., 2014; Sieracki and Viles, 1992; Yamasaki et al., 1998). ONAP is an important organic carbon reservoir in coastal and oceanic waters, thus they are responsible of modulating several biogeochemical processes linked to carbon (e.g., heterotrophic bacteria respiration, carbon export) (Bauerfeind, 1985; Segschneider and Bendtsen, 2013; Turner, 2015) and nitrogen cycles (e.g., denitrification) (Eyre et al., 2013). Thus, ONAP dynamics affects ecosystem function and structure, and is influenced by climate-mediated changes on environmental variables (Nixon et al., 2009; Kelaher et al., 2013).

NAP represents a major biogeochemical component affecting inherent optical properties (IOPs) of littoral waters (Babin et al., 2003). Thus, the characterization of ONAP optical properties is fundamental for optical closure analysis, development/validation of remote sensing models, and interpretation of ocean color signal arriving to the satellite sensor. Optical properties of NAP are very different between locations and periods of the year due to variations in particle chemical composition, porosity, size distribution (PSD) and shape (Green et al., 2008; Neukerman et al., 2012). The effect of NAP on IOPs variability is mainly attributed to changes on scattering (Stramski et al., 2004). In coastal waters, simulations based on Mie theory suggest that ONAP and mineral particulates may account for most of the scattering coefficient variability in the backward direction (Green et al., 2003).

Table 1. List of acronyms

Parameter	Definition	Units
SLE	St Lawrence Estuary	
NAP	non-algal particulates	

ONAP	Organic non-algal particulates	
TP	<i>Thalassiosira pseudonana</i>	
DT	<i>Dunaliella tertiolecta</i>	
SLE	Saint Lawrence Estuary	
IOPs	Inherent optical properties	
PSD	Particle size distribution	
CDOM	Colored dissolved organic matter	
Chl	chlorophyll a concentration	mg m ⁻³
chl/C	chlorophyll a-to-particulate Carbon ratio	dimensionless
[PIM]	particulate inorganic matter concentration	g m ⁻³
[POM]	particulate organic matter concentration	g m ⁻³
[POM ^{phyto}]	concentration of POM associated to phytoplankton	g m ⁻³
[POM ^{ONAP}]	concentration of POM associated to ONAP	g m ⁻³
[POC ^{phyto}]	concentration particulate organic carbon associated to phytoplankton	g m ⁻³
f1	[POC ^{phyto}]/chl ratio	dimensionless
f2	[POM ^{phyto}]/[POC ^{phyto}] ratio	dimensionless
λ	Wavelength	nm

A	total absorption coefficient	m^{-1}
a_w	absorption coefficient of pure seawater	m^{-1}
a_p	absorption coefficient of particulates	m^{-1}
a_{ph}	absorption coefficient of phytoplankton	m^{-1}
a_{nw}	absorption coefficient of phytodetritus suspensions	m^{-1}
a_{CDOM}	absorption coefficient of chromophoric dissolved organic matter	m^{-1}
a_{NAP}	absorption coefficient of NAP	m^{-1}
a_{NAP}^*	mass-specific absorption coefficient of NAP	m^{-1}
a_{ONAP}	absorption coefficient of ONAP	m^{-1}
a_{ONAP}^*	mass-specific absorption coefficient of ONAP	$\text{m}^{-2} \text{ g}^{-1}$
a_{POM}	absorption coefficient of POM	m^{-1}
a_{POM}^*	mass-specific absorption coefficient of POM	m^{-1}
a_{PIM}	absorption coefficient of PIM	m^{-1}
a_{PIM}^*	mass-specific absorption coefficient of PIM	m^{-1}
a_p^*	mass-specific absorption coefficient of particulates	$\text{m}^2 \text{ g}^{-1}$
a_{ph}^*	mass-specific absorption coefficient of phytoplankton	$\text{m}^2 \text{ g}^{-1}$
a_{diss}	absorption coefficient of dissolved matter after filtering through 0.7 μm membranes	m^{-1}

b_{diss}	scattering coefficient of dissolved matter after filtering through 0.7 μm membranes	m^{-1}
c_{diss}	beam attenuation coefficient of dissolved matter after filtering through 0.7 μm membranes	m^{-1}
c_{nw}	beam attenuation coefficient of phytodetritus suspensions	m^{-1}
c_p	beam attenuation coefficient of particulates	m^{-1}
c_{ph}	beam attenuation coefficient of phytoplankton	m^{-1}
b_p^*	mass-specific scattering coefficient of particulates	$\text{m}^2 \text{g}^{-1}$
B	total scattering coefficient	m^{-1}
b_w	scattering coefficient of pure seawater	m^{-1}
b_{nw}	scattering coefficient of phytodetritus suspensions	m^{-1}
b_p	scattering coefficient of particulates	m^{-1}
b_{ph}	scattering coefficient of phytoplankton	m^{-1}
b_{ONAP}	scattering coefficient of ONAP	m^{-1}
b_{ONAP}^*	mass-specific scattering coefficient of ONAP	$\text{m}^{-2} \text{g}^{-1}$
c_{ONAP}	beam attenuation coefficient of ONAP	m^{-1}
b_{POM}	scattering coefficient of POM	m^{-1}
b_{PIM}	scattering coefficient of PIM	m^{-1}

σ_c^{bact}	attenuation cross section of heterotrophic bacteria	$\text{m}^2 \text{ cell}^{-1}$
σ_a^{HB}	absorption cross section of heterotrophic bacteria	$\text{m}^2 \text{ cell}^{-1}$
σ_b^{HB}	scattering cross section of heterotrophic bacteria	$\text{m}^2 \text{ cell}^{-1}$
N_{HB}	number of heterotrophic bacteria	counts m^{-3}
a_{HB}	absorption coefficient of heterotrophic bacteria	m^{-1}
b_{HB}	scattering coefficient of heterotrophic bacteria	m^{-1}
c_{HB}	beam attenuation coefficient of heterotrophic bacteria	m^{-1}
VSF	Volume scattering function	$\text{m}^{-1} \text{ sr}^{-1}$

Unlike inorganic particulates, the optical characterization of ONAP based on *in situ* measurements is challenging given the difficulties on separating organic from mineral fractions in ‘bulk’ samples. Specific methods for concentrating organic detritus derived from field samples (e.g., glucose density gradients) (Hamilton et al., 2005) are not suitable for optical determinations due to the alteration of IOPs during the centrifugation process. Thus, several studies have been focused in measuring the optical properties of individual ONAP particles (e.g., microphotography, flow cytometry) (Iturriaga and Siegel, 1989; Yentsch and Yentsch, 2008). In general, these studies agree regarding the greater importance of scattering with respect to absorption and the higher absorption of ONAP toward the ultraviolet spectral range. The absorption of ONAP has been principally attributed to chromophores derived from heterotrophic microbes and pigment degradation products (Nelson, 1993; Nelson and Robertson, 1993).

Current biogeo-optical models used in remote sensing studies do not discriminate organic from inorganic fractions of NAP. Also, the light absorption due to NAP and chromophoric dissolved organic matter (CDOM) is usually parameterized using a common term due to the difficulty on teasing out these optical signatures (Gordon et al., 2009; Cael and Boss, 2017). Given the technical limitations of operational ocean color sensors (e.g., lack of ultraviolet channels, poor calibration of polarized channels) (Tilstra and Stammes, 2007; Wei and Lee, 2015), the discrimination of ONAP based on optical remote sensing information is not feasible yet. However, if satellite-retrievals of NAP-related IOPs are obtained (e.g., absorption coefficient) (Gohin, 2011) and *in situ* measurements of particulate inorganic matter (PIM) are available, models based on mass-specific optical coefficients (Stavn and Richter, 2008) can be proposed *a posteriori* to separate NAP optical contributions due to organic and inorganic matter. To our understanding, the calculation of mass-specific absorption and scattering coefficients of ONAP (a_{ONAP}^* and b_{ONAP}^* , respectively) has never been reported.

The St Lawrence Estuary (SLE) is a large sub-arctic coastal system characterized by major pulses of freshwater derived from the St Lawrence River and tributaries mainly located along the northern shore (e.g., Saguenay River, Outardes River) (Saucier et al., 2009). The SLE waters are optically complex (i.e., variability of IOPs is dominated by multiple components such as phytoplankton, NAP and CDOM) (Nieke et al., 1997). In general, NAP contribution to IOPs increases upstream and near the mouth of streams situated along the northern shore of the SLE (Montes-Hugo et al., 2012; Montes-Hugo and Xie, 2015).

This study has three objectives: 1) to determine the spectral absorption and scattering coefficients (i.e., wavelength range = 412-710 nm) of organic detritus (hereafter a_{ONAP} and b_{ONAP} , respectively) derived from two phytoplankton cultures (*Thalassiosira pseudonana* and *Dunaliella tertiolecta*, TP and DT, respectively), 2) to compute the spectral a_{ONAP}^* and b_{ONAP}^* values for each type of phytodetritus and relate these mass-specific optical

coefficients to their PSDs, and 3) to estimate the optical contribution of organic detritus to particulate absorption and scattering measurements made in surface waters (i.e., 0-10 m depth) of the SLE during May 2010 and June 2011.

The results of this study are organized in four sections. Firstly, lab experiments related to the production of phytodetritus are described in detail. Secondly, measurements of a_{ONAP} and b_{ONAP} are corrected due to contamination associated to heterotrophic bacteria. Also, optical and gravimetric measurements of phytodetritus are combined to obtain a_{ONAP}^* and b_{ONAP}^* values. Thirdly, the variability of optical properties of TP- and DT-derived detritus is related to changes on PSD. Lastly, empirical biogeo-optical models are used to simulate optical coefficients of organic detritus in samples obtained in the SLE during May 2000 and April 2001. The spectral variability of lab-derived and modeled coefficients of ONAP was compared, and regional changes of modeled optical coefficients were related to environmental variables (e.g., river discharge, wind speed).

1.4 MATERIALS AND METHODS

1.4.1. LAB MEASUREMENTS

Phytodetritus

Strains of TP and DT were obtained from the collection of marine phytoplankton at the Provasoli-Guillard National Center for Marine Algae and Microbiota, Bigelow laboratory (diatom CCMP1335, chorophyceae, CCMP1320). These phytoplankton species were selected as ‘models’ of phytoplankton producing phytodetritus in the SLE due to several reasons: 1) they have been used previously in detritus experiments (Romann, 1984; Biddanda and Pomeroy, 1988; Williams et al., 1995; Verity et al., 1996; Verity et al., 2000), 2) they are relatively easy to cultivate, 3) they have contrasting characteristics in terms of shape, size and chemical composition (Tomas, 1997), 4) their living cells have been optically characterized (Stramski and Reynolds, 1993; DuRand and Olson, 1998), and 5)

they represent main phytoplankton groups of the SLE (i.e., ‘diatoms’ and flagellates) (Roy et al., 2008).

The phytoplankton culture medium of DT was prepared with a standard mineral composition based on f/2 recipe. Silica requirements of TP were met by enriching the original f/2 medium formulation with Na_2SiO_3 . The medium f/2 was prepared with filtered seawater (pore size = 0.2 μm , Nucleopore) collected from surface waters of the lower part of the SLE. This filtration step eliminates most of detritus, however optical studies suggest that a minor colloidal residual fraction may be still present (Zhang et al., 2011). To eliminate bacterial contamination during the preparation of the culture media, the f/2 solutions were autoclaved at 120°C and during 20 minutes before the experiments. The incubations were done at 15°C in a temperature controlled room and using fluorescent light ($250 \mu\text{mol m}^{-2} \text{s}^{-1}$ within the visible spectral range with a photoperiod of 14:10 light: dark cycle.

The production of phytodetritus encompassed five steps. In step 1, phytoplankton culture samples (20 ml each) were obtained in 50 ml plastic tubes and during the senescent growth phase of the microalgae (i.e., 5 weeks after the culture initiation). In step 2, the samples were frozen and kept at -20°C during 24 h. In step 3, frozen samples were thawed, resuspended in 500 ml of filtered seawater (pore size = 0.2 μm , Nucleopore), exposed to ultrasound during 30 seconds (Ultrasonic Processor XL 2010), and subsequently stored in dark conditions and room temperature (i.e., 20°C). The sonication had a power of 10 W and was performed 3 times inside an ice-bath in order to avoid temperature degradation effects. In step 4, each sonicated sample was diluted using 3.5 L of Nanopure water before performing the bench optical measurements (see section 2.1.3). Lastly in step 5, 10 ml of phytodetritus samples were concentrated using fiber glass membranes (pore size = 0.7 μm , GF/F, Whatman). The filtrate was subsequently filtrated through a polycarbonate membrane (pore size = 0.2 μm , Nucleopore, Whatman). The material retained in both

filters was extracted with 90% acetone during 24 h, in dark conditions and at 5°C. Fluorescence measurements of extracts were performed by triplicate using a fluorometer (AU Turner 10-AU). Pigment concentrations were determined by the non-acidification technique (Welschmeyer, 1994). Lastly, the steps 2 to 5 were repeated till the concentration of chlorophyll a per unit of volume (chl) was unchanged (i.e., variation between cycles less than 5%). The step 5 was critical to verify the efficiency of the cell breakage due to freezing-thawing and sonication treatments. The decrease of chlorophyll fluorescence is an indicator of chlorophyll degradation, a process that is only possible when cell membranes are disrupted.

Contamination of phytodetritus due to bacteria

Original phytoplankton strains used in this study are expected to be axenic, however bacterial contamination is likely to occur during the initial culture and each stage of cell destruction described above. Although the definition of organic detritus in field measurements includes bacteria, here the bacteria contribution to ONAP is considered an external contamination caused by different factors related to the sample manipulation (e.g., non-sterile ultrasound probe, etc). Since bacteria explain a substantial fraction of particulate scattering coefficients in aquatic systems (Stramski and Kiefer, 1991; Stramski et al., 2001; Montes-Hugo et al., 2009), the optical contribution of bacteria to organic detritus must be removed.

The abundance of heterotrophic bacteria (free living + attached) was determined before and after the optical measurements using the ac-9 instrument and following the method proposed by Porter and Freig (1980). Firstly, a volume of 10 ml was quickly fixed with 1 ml of glutaraldehyde 25% and during 5 minutes. A posteriori, 100 µml of DAPI (4',6-diamidino-2-phenylindole) solution (1 mg ml^{-1}) was added to the sample. The staining lasted 15 minutes and was made under dark conditions. Lastly, 2 ml of sample was filtered

through a black Nucleopore polycarbonate filter (pore size = 0.2 μm), and bacteria was enumerated by using an epifluorescence microscope (Olympus BX41) configurated with a 100x silicon oil immersion objective (Sieracki et al., 1985; Smith and Azam, 1992). Each bacteria abundance estimate corresponded to the arithmetic average of 100 determinations (5 samples x 20 fields).

The absorption (a_{HB}) and beam attenuation (c_{HB}) coefficients of heterotrophic bacteria were computed based on optical cross sections reported by Stramski and Kiefer (1990) for heterotrophic bacteria cultures:

$$a_{\text{HB}} = \sigma_a^{\text{HB}} N_{\text{HB}} \quad (1)$$

$$c_{\text{HB}} = \sigma_c^{\text{HB}} N_{\text{HB}} \quad (2)$$

where σ_a^{HB} and σ_c^{HB} are the mass-specific optical cross sections for absorption and beam attenuation coefficients in cell m^{-2} , respectively. N_{HB} is the abundance of bacteria per unit of volume (cell m^{-3}). The scattering coefficient of heterotrophic bacteria (b_{HB}) was calculated by subtracting a_{HB} from c_{HB} .

Optical measurements

Absorption (a_{nw}) and beam attenuation (c_{nw}) coefficients of phytodetritus suspensions (i.e., phytodetritus + CDOM) were measured with an absorption-attenuation meter (ac-9, WetLabs, spectral resolution = 10 nm, precision $\pm 0.003 \text{ m}^{-1}$) at nine wavelengths ($\lambda = 412, 440, 488, 510, 532, 555, 650, 676$, and 715 nm). The scattering coefficient of phytodetritus suspensions (b_{nw}) was computed by substracting a_{nw} from c_{nw} values. Notice that initial ac-9 measurements do not include the optical contribution due to pure seawater since it is initially removed by the manufacturer during the instrument calibration. Due to drift of ac-9 measurements (Twardowski et al., 1999), a baseline adjustment was performed before the sample measurements by using Nanopure water. This correction was important to eliminate the bias on optical measurements associated to changes on instrument noise and lab

temperature. The errors of optical measurements due to multiple scattering effects were minimized by applying the proportional method of Zanaveld et al. (1994). Briefly, this technique assumes that absorption in the near infrared region is zero and the volume scattering function is spectrally-independent. The scattering corrected absorption coefficient is computed by subtracting the value at 715 nm and multiplying that value by a spectral factor that is proportional to the total scattering (McKee et al., 2013). Multiple scattering effects occur inside the ‘a’ (i.e., absorption tube) and the ‘c’ (i.e., beam attenuation tube) tubes due to the incomplete reflection of photons against the wall of the reflective tube and the partial exclusion of forward-scattered photons inside the opaque tube (McKee et al., 2008). An incomplete correction of these effects led to an overestimation of absorption and an underestimation of scattering coefficients of phytodetritus, respectively.

The circulation of water through the ac-9 tubes was done manually by flushing the tubes using gravity. Each sample measurement lasted 3 minutes and had a sampling frequency of 1 Hz. The optical contribution of CDOM to phytodetritus suspensions was eliminated from a_{nw} and c_{nw} values by subtracting the optical measurements made with pre-filtered samples (GF/F membrane, pore size = 0.7 μm) in ‘a’ (a_{diss}) and ‘c’ (c_{diss}) tubes, respectively. Notice that a_{diss} and c_{diss} estimates have contamination due to free-living bacteria (i.e., organisms generally smaller than 1 μm). The optical contribution of particle-attached bacteria to a_{nw} and c_{nw} coefficients was removed by subtracting the a_{HB} and c_{HB} values associated to particle-attached bacteria (i.e., total x particle-attached/total averaged factor) (Montes-Hugo et al., 2007). The resulting optical coefficients correspond to bacteria-free absorption, attenuation and scattering coefficients of phytodetritus (hereafter a_{ONAP} , c_{ONAP} and b_{ONAP} , respectively)

The mass-normalized absorption and scattering coefficients of phytodetritus (hereafter a_{ONAP}^* and b_{ONAP}^* , respectively) were obtained by normalizing a_{ONAP} and b_{ONAP} measurements by the dry weight of particulate material retained in GF/F fiber glass

membranes (pore size = 0.7 µm, Whatman). Final weights were adjusted by removing the microbial mass associated to bacteria contamination and assuming a weight per bacteria of $10 \cdot 10^{-12}$ g (Cermak et al., 2016). The dry weight of phytodetritus was quantified using an analytical balance Sartorius (accuracy ± 0.0001 g).

The size distribution of organic detritus was estimated based on optical microscopy after labeling the particulates with DAPI (Mostajir et al., 1995). A total of 100 samples of 0.05 ml were analyzed. Particles were counted using a grid and an objective of 60x. The diameter of each particle corresponds to the largest axis and was computed using the image processing software ImageJ (Schneider et al., 2012).

1.4.2. *In situ* datasets

Study area and sampling design

The SLE is the largest estuarine system in the world (El Sabh, 1979), and is characterized by two regions (the upper and lower estuary) having contrasting bottom depths (< 30 m and up to 350 m, respectively) (Sundby, 1974; Yeats, 1988) (Fig. 1). The suspended particulate matter in the SLE is mainly composed by inorganic matter (up to 95%) (D'Anglejan and Smith, 1973).

Surveys of optical and biogeo-chemical properties were conducted in surface waters (i.e., 1.5 m depth) of the Saint Lawrence Estuary during 17-31 May of 2000, and from 20 April to 4 May of 2001 (Fig. 1). These optical datasets were chosen because they were the only historical archive available during this thesis. Sampling periods coincided with the spring freshet (freshwater discharge up to $20 \cdot 10^3 \text{ m}^3 \text{ s}^{-1}$) (Pêches et Oceans Canada, Hydro-Quebec). In all cases, discrete water samples for biogeo-optical measurements were obtained with go-Flo bottles (5 L).

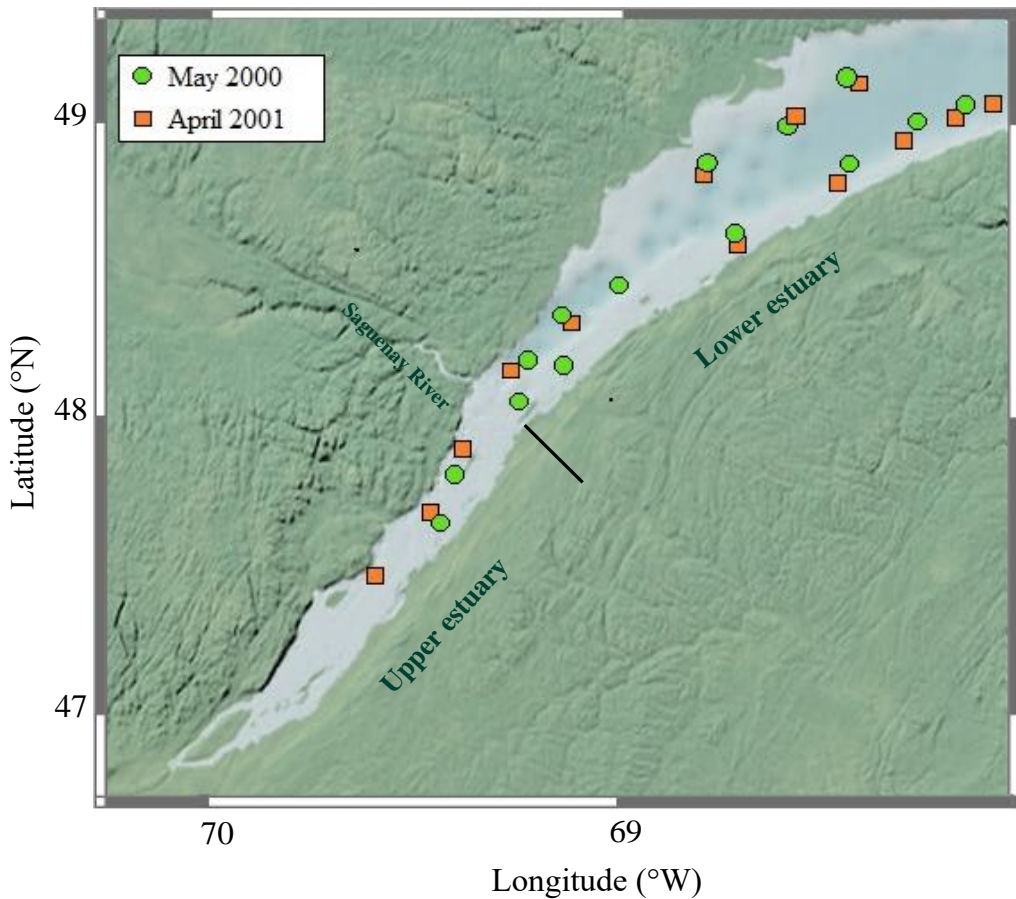


Fig. 1. Study area. Sampling locations during May 2000 (green circles) and April 2001 (orange rectangles) cruises.

Optical measurements

Vertical profiles of absorption (a) and beam attenuation (c) coefficients were made using an absorption-attenuation meter (ac-9, path-length = 25 cm, wavelengths = 412, 440, 488, 510, 532, 555, 650, 676, and 715 nm, sampling rate = 6 Hz, WetLabs). Deionized water (Barnstead NANO purewater purification unit) was used as a baseline to correct the instrument drift as a function of time. Particulate absorption (a_p) and attenuation (c_p) coefficients were calculated from total absorption and attenuation coefficients by

subtracting the contribution of CDOM and eliminating multiple scattering effects due to particulates (Zaneveld et al., 1994). The absorption and attenuation due to CDOM was measured by pre-filtering the sample through a Nucleopore membrane (pore = 0.2 µm, Whatman) (Twardowski et al., 1999). The particulate scattering coefficient (b_p) was calculated by subtracting a_p from c_p . Final estimates of a_p , b_p and c_p were corrected by salinity-temperature differences between the calibration and *in situ* temperature (Pegau and Zanaveld, 1993).

The phytoplankton absorption coefficient (a_{ph}) was derived from spectrophotometric measurements and following the filter-pad technique (Mitchell et al., 2002). Discrete water samples for the absorption coefficient of particulates were filtered trough GF/F membranes (pore size = 0.7 µm, Whatman). Filtered samples were stored in dry, cool and dark conditions before performing absorbance measurements using a Perkin Elmer Lambda 2 spectrophotometer (wavelength range = 190-1100 nm, spectral resolution = 0.3 nm, precision ± 0.005). The absorption coefficient of NAP (a_{NAP}) was determined by repeating the same measurement after extracting the pigments with Methanol (Kishino et al., 1985). The magnitude of a_{ph} was computed by subtracting a_{NAP} from a_p values.

Biogeo-chemical measurements

Discrete water samples for PIM and particulate organic matter (POM) were filtered through pre-weighted and dry GF/F membranes (pore size = 0.7 µm, Whatman) (Strickland and Parson, 1972). At the end of each filtration, filters were rinsed with deionized water to remove sea salts. PIM was obtained after removing the organic mass by combustion at 450°C and during 6 h. The precision of mass determinations for total particulates was 15% (Mohammadpour et al., 2015). This error was larger for PIM (~18%) due to the dehydration of clays (Barillé-Boyer et al., 2003; Mohammadpour et al., 2017).

The analysis of chlorophyll was done based on fluorometry and using the acidification technique (Strickland and Parsons, 1972). Briefly, a volume of water (0.5 L) was filtered using GF/F membranes, and filtered samples were stored during 72 h in liquid nitrogen. A posteriori, pigments on samples were extracted in cold (i.e., 4-5°C) 90% acetone and under dark conditions during 24. Lastly, the fluorescence of extracted samples was measured in the lab at constant temperature by using a fluorometer TD-10AU Turner Designs (precision ± 4%). The signal interference due to phaeopigments was corrected in two steps: 1) a second fluorescence reading is done after adding 2 drops of diluted HCl (2%) to the original sample, and 2) the fluorescence of the acidified sample is subtracted from the first measurement (i.e., without acidification).

Biogeo-optical models of ONAP

The absorption and scattering coefficients of organic detritus were modeled based on published parameterizations and *in situ* measurements obtained in the SLE during the oceanographic cruises described in section 2.2.1.

First, the concentration of particulate POM associated to ONAP ($[POM^{ONAP}]$) was calculated as follows:

$$[POM^{phyto}] = chl \times f1 \times f2 \quad (3)$$

$$[POM^{ONAP}] = [POM] - [POM^{phyto}] \quad (4)$$

where $[POM^{phyto}]$ is the concentration of particulate organic matter associated to phytoplankton in g m^{-3} . The factor f1 is 50 and corresponds to $[POC^{phyto}]/chl$ or the average ratio between the concentration of particulate organic carbon associated to phytoplankton ($[POC^{phyto}]$) and chl (Behrenfeld et al., 2005). The factor f2 varied between 1.34 and 1.55 and represents the $[POM^{phyto}]/[POC^{phyto}]$ ratio and was computed based on field measurements obtained during May 2000 and April 2001 cruises. The ratio $[POM^{phyto}]/[POC^{phyto}]$ assumes that phytoplankton and non-phytoplankton organic particulates have the same mass contribution of POC to POM.

The absorption and scattering coefficient of POM (hereafter a_{POM} and b_{POM} , respectively) were calculated by subtracting the contribution of inorganic matter from a_p and b_p values, respectively. The absorption coefficient of inorganic particulates (a_{PIM}) was derived at each wavelength by multiplying the mass-specific absorption coefficient of PIM (a_{PIM}^*) by the PIM concentration. An average spectral curve of a_{PIM}^* ('brown earth') was chosen based on measurements made in coastal waters having a comparable turbidity to the SLE (e.g., Irish Sea) (Ahn, 1990). Values of a_{PIM}^* for the spectral range 400-750 nm vary between 0.02 and $0.14 \text{ m}^2 \text{ g}^{-1}$.

The mass-specific absorption coefficient of POM was computed as follows:

$$a_{\text{POM}}^* = a_{\text{POM}} / [\text{POM}] \quad (5)$$

where a_{POM} is derived by subtracting a_{PIM} from a_p values and $[\text{POM}]$ is the concentration of total particulate organic matter in g m^{-3} . The absorption coefficient of organic detritus was simulated by using the following expression:

$$a_{\text{ONAP}} = a_{\text{POM}}^* [\text{POM}] - a_{\text{ph}}^* \text{ chl} \quad (6)$$

where a_{ph}^* is the regionally-weighted and chl-specific absorption coefficient of phytoplankton ($\text{m}^2 \text{ mg}^{-1}$) as computed from field samples obtained during May 2000 and April 2001 cruises.

Similar to a_{ONAP} , the calculation of b_{ONAP} included two steps, the removal of the inorganic matter contribution to particulate scattering coefficient and the removal of phytoplankton contribution to b_{POM} :

$$b_{\text{POM}} = b_p - b_{\text{PIM}}^* [\text{PIM}] \quad (7)$$

$$b_{\text{ph}} \cong B1 \times \text{chl}^{0.62} \times (550/\lambda) - b_w \quad (8)$$

$$b_{\text{ONAP}} = b_{\text{POM}} - b_{\text{ph}} \quad (9)$$

where b_{PIM}^* is the mass-specific scattering coefficient of PIM in $\text{m}^2 \text{ g}^{-1}$, b_{ph} is the scattering coefficient of phytoplankton in m^{-1} , $[\text{PIM}]$ is the concentration of PIM in g m^{-3} , $B1$ is an averaged coefficient equal to 0.3 that varies between 0.12 and 0.45 at $\lambda = 550 \text{ nm}$ (Gordon and Morel, 1983), and b_w is the scattering coefficient of pure seawater in m^{-1} (Morel, 1974).

The empirical model in equation (8) corresponds to oceanic waters and does not include very oligotrophic environments (Gordon and Morel, 1983). Thus, NAP covary with phytoplankton (i.e., case I waters), IOPs are dominated by phytoplankton, and optical contribution of NAP is negligible (i.e., <10%). Lastly, the b_{PIM}^* curve was derived from the Hydrolight optical database and corresponds to coastal 'brown earth' particulates (Ahn, 1990). Values of b_{PIM}^* vary between 0.57 and 0.67 $\text{m}^2 \text{ g}^{-1}$ for the spectral range 400-750 nm. Similar to a_{PIM} curves, b_{PIM} curves derived from 'brown earth' measurements are widely used for modeling optically complex (Mobley, 1995). Mass-specific coefficients of a_{ONAP} and b_{ONAP} (hereafter a_{ONAP}^* and b_{ONAP}^* , respectively) were calculated by normalizing absorption and scattering coefficient estimates by $[\text{POM}^{\text{ONAP}}]$ values computed in equation (4).

1.5 RESULTS

1.5.1. Lab measurements

1.5.1.1. Optical properties of phytodetritus

Chlorophyll a concentration during the exponential, stationary and senescent growth phases of TP and DT cultures was measured at day 10, 15 and 30 after the inoculation of the medium, respectively. The average of chl for each one of these sampling periods was always higher for DT (14.12 ± 0.20 , 16.20 ± 0.15 , and $8.45 \pm 0.19 \text{ mg m}^{-3}$, arithmetic average \pm standard error or se) with respect to TP (11.23 ± 0.22 , 13.40 ± 0.24 , and $6.12 \pm 0.17 \text{ mg m}^{-3}$) samples. Phytoplankton abundance for the senescent phase of DT and TP cultures was $7.8 \cdot 10^6$ and $3.5 \cdot 10^6 \text{ cells ml}^{-1}$, respectively.

Lab experiments showed that efficiency on producing phytodetritus varied between phytoplankton species (Fig. 2). Despite the higher initial fluorescence of DT with respect to TP fragments (~1.3 fold), both types of phytodetritus had a comparable fluorescence 20 days after exposing the samples to temperature and sonication treatments. Thus, the rate of

change of fluorescence, an indicator of phytodetritus production efficiency, was higher for DT- ($0.56 \text{ mg chlorophyll m}^{-3} \text{ d}^{-1}$) than TP-derived detritus ($0.43 \text{ mg chlorophyll m}^{-3} \text{ d}^{-1}$). In day 1, the fluorescence decrease due to cell breakage was 92% and 94% for DT and TP, respectively.

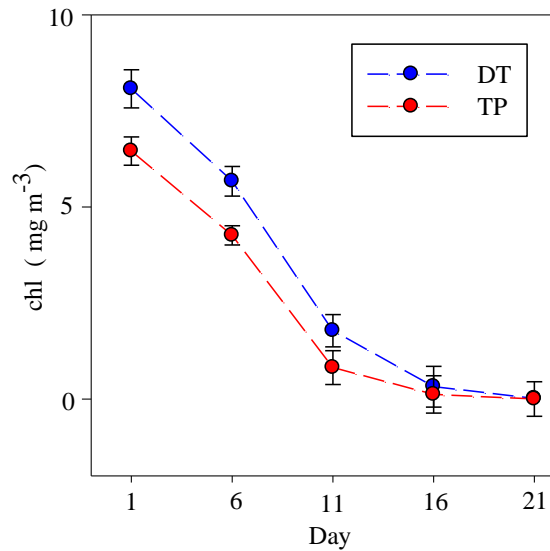


Fig. 2. Phytoplankton cell disruption due to thermal and acoustic stress. Chlorophyll a concentration in DT (blue symbols) and TP (red symbols) samples collected during the senescent growth phase and treated at different time lags. Uncertainty bars indicate two standard errors

The fluorescence of fragments of both phytoplankton species was not statistically different at 95% confidence level and with respect to the blank (i.e., chl = 0) after two weeks of sonication/temperature treatments. The optical interference due to heterotrophic bacteria contamination occurred in both types of phytodetritus and was relatively small (i.e., contribution to a_{ONAP} and b_{ONAP} less than 6%, at $\lambda = 412 \text{ nm}$) (Fig. 3).

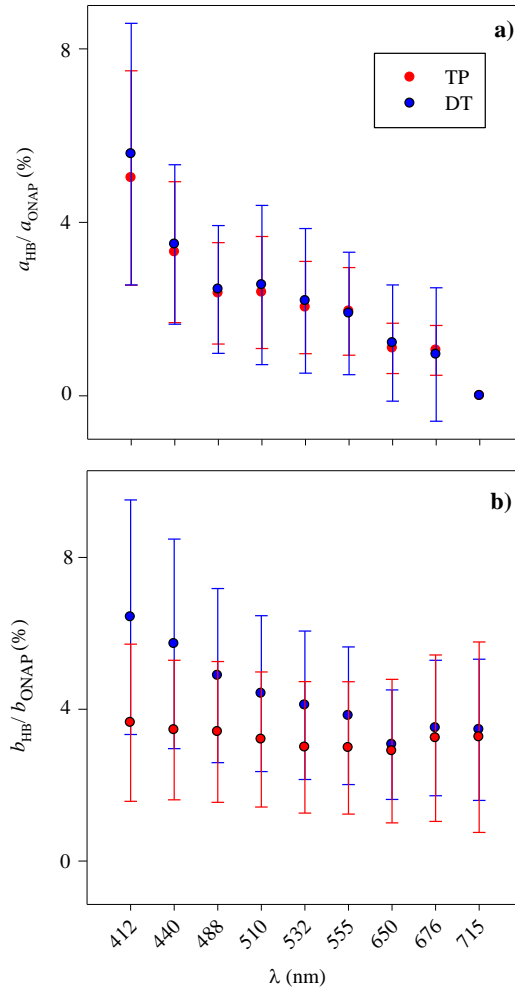


Fig. 3. Optical contribution of heterotrophic bacteria to spectral absorption and scattering coefficients of phytodetritus. a) a_{HB}/a_{ONAP} , and b) b_{HB}/b_{ONAP} . DT (blue symbols) and TP (red symbols), contributions in percentage. Uncertainty bars indicate two standard errors.

In general, DT had a greater abundance of bacteria before ($4.23 \pm 0.39 \text{ } 10^7 \text{ cells ml}^{-1}$) and after ($4.87 \pm 0.22 \text{ } 10^7 \text{ cells ml}^{-1}$) the ac-9 measurements with respect to TP phytodetritus samples ($3.12 \pm 0.11 \text{ } 10^6$ and $3.47 \pm 0.15 \text{ } 10^6 \text{ cells ml}^{-1}$, respectively). Notice that bacteria abundance for each type of phytodetritus corresponded to the average of two determinations made within 15 minutes.

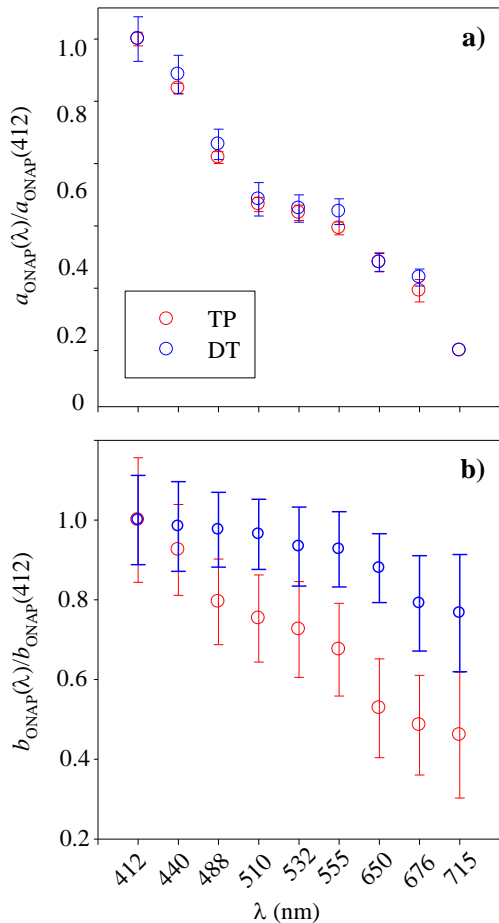


Fig. 4. Spectrally-normalized optical coefficients of phytodetritus. a) particulate absorption, and b) particulate scattering; DT (blue symbols) and TP (red symbols), contributions in percentage. Uncertainty bars indicate two standard errors.

The contribution of heterotrophic bacteria to the absorption coefficient of TP and DT phytodetritus was comparable ($P > 0.05$) and tended to increase at shorter wavelengths (Fig. 3a). The contribution of heterotrophic bacteria to the scattering coefficient of phytodetritus tended to be larger for DT samples even though substantial changes could not be demonstrated due to the large uncertainties of estimates (Fig. 3b).

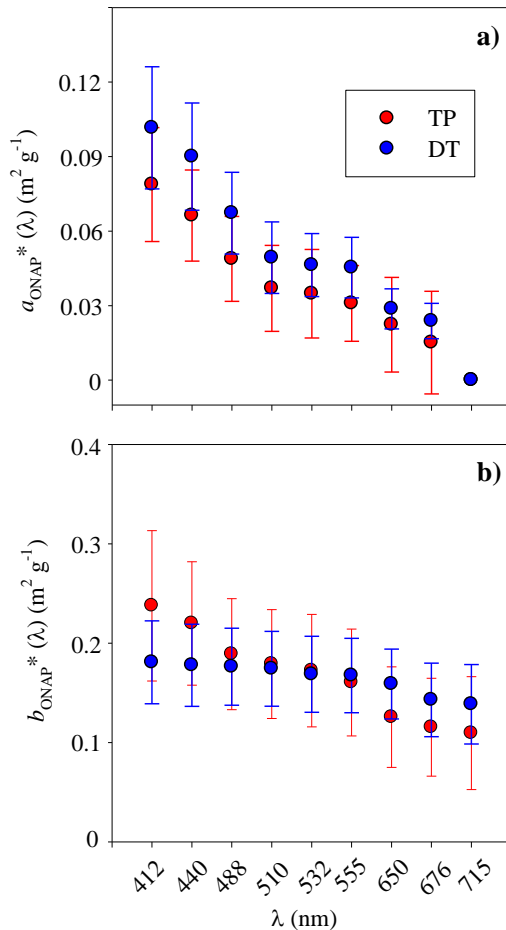


Fig. 5. Mass-specific absorption and scattering coefficients of phytodetritus. a) particulate absorption, and b) particulate scattering; DT (blue symbols) and TP (red symbols), contributions in percentage. Uncertainty bars indicate two standard errors.

Spectral curves of lab-derived a_{ONAP} and b_{ONAP} values normalized at a wavelength of 412 nm and for two types of phytodetritus are shown in Figure 4.

The spectral variation of absorption coefficients of phytodetritus derived from TP and DT cultures was not substantially different and consistently agreed with a higher absorption a

shorter wavelengths (Fig. 4a). The increase of normalized values of scattering coefficients of ONAP at shorter wavelengths was also observed in both types of phytodetritus (Fig. 4b), However, the shape of normalized curves suggested a larger relative scattering at longer wavelengths than 488 nm for phytodetritus samples derived from DT.

The mass-normalized absorption coefficients of DT-derived phytodetritus were commonly higher with respect to those calculated for detritus originated from TP even though no statistical differences were detected at 95% confidence level (Fig. 5a). Also, the large uncertainty of mass-normalized scattering coefficients made difficult the differentiation between different types phytodetritus (Fig. 5b). The arithmetic average of a_{ONAP}^* at a wavelength of 440 nm was 0.092 and $0.066 \text{ m}^2 \text{ g}^{-1}$ for DT and TP, respectively. Likewise, The arithmetic average of b_{ONAP}^* at a wavelength of 555 nm was $0.16 \text{ m}^2 \text{ g}^{-1}$ for both types of phytodetritus.

1.5.2. Size distribution of phytodetritus

Most detrital particles derived from TP and DT samples were counted within the smallest size bins (e.g., 61 and 67% of DT and TP particles, respectively, had a size range of 0.6-1.4 μm) (Fig. 6). The slope of log-normal PSD was comparable for DT- (-114.9 ± 68.4 , 2 standard errors) and TP-derived (-137.9 ± 72.2) detritus even though DT was characterized by a greater number of particles in the size bins having the largest diameters (i.e., $> 2.6 \mu\text{m}$).

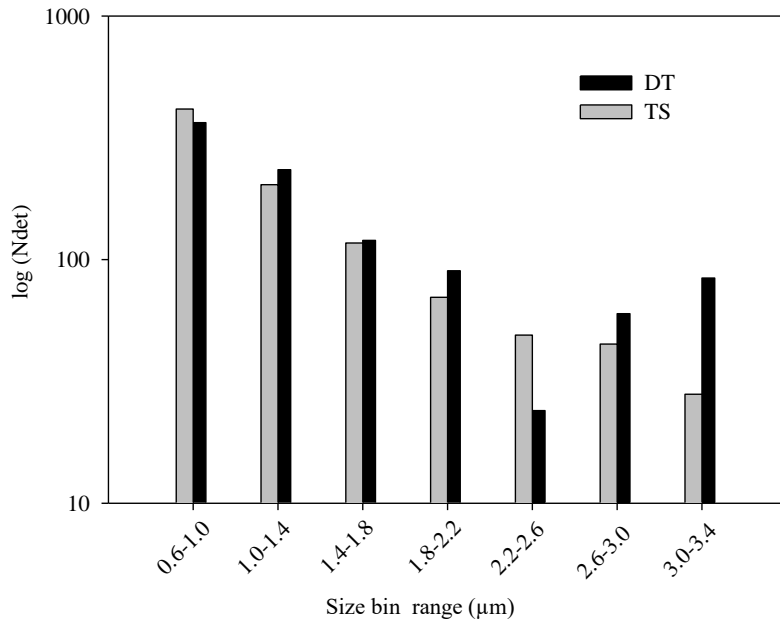


Fig. 6. Particle size distribution of phytodetritus. Log-transformed number of detrital particles (Ndet) based on 100 microscope fields and for different particle size bins (x-axis). DT- (solid black) and TD-derived detritus (solid grey).

The weighted arithmetic average of phytodetritus diameter for DT and TP samples was 1.47 and 1.33 μm , respectively. The size of these particles represents 21 and 27% of the averaged size of DT (3-12 μm) and TP (4-6 μm) living cells, respectively.

1.5.3. Field measurements

Absorption and scattering coefficients of organic detritus calculated with samples obtained in the SLE during May 2000 and April 2001 are shown in Figure 7. During the two periods of study, the magnitude of a_{ONAP} estimates decreased at longer wavelengths. This pattern was also present for spectral simulations of b_{ONAP} at wavelengths shorter than 555 nm and based on data collected during April 2001. The arithmetic average of $a_{ONAP}(440)$ computed over the SLE was not substantially different between surveys (0.76 ± 0.83 (2 se) and 0.60 ± 0.92 m^{-1} for May 2000 and April 2001 cruises, respectively)

(Fig. 7a). The regional arithmetic average of $b_{ONAP}(555)$ was $0.27 \pm 1.77 \text{ m}^{-1}$ for samples obtained during April 2001 (Fig. 7b).

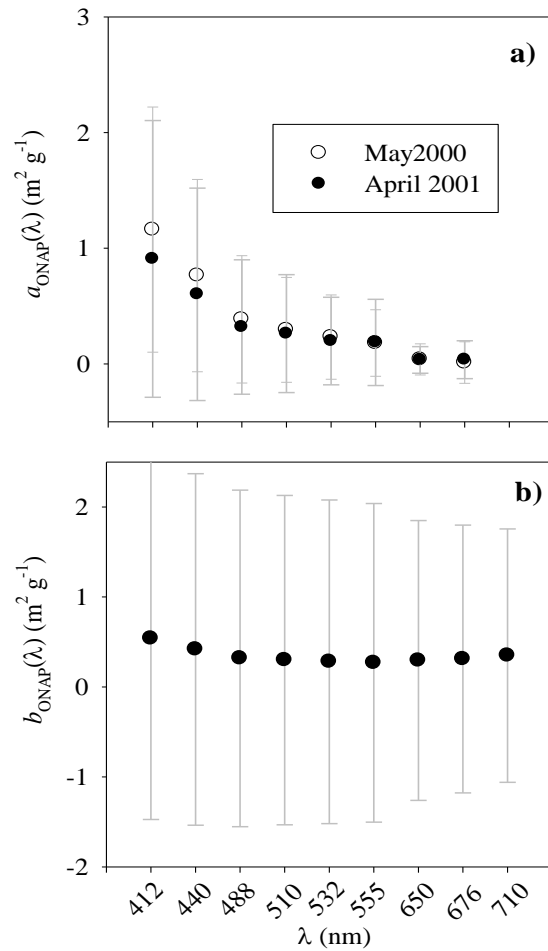


Fig. 7. Modeled spectral absorption and scattering coefficients of ONAP in the SLE. a) particulate absorption, and b) particulate scattering; May 2000 (empty circles), April 2001 (solid circles). Uncertainty bars indicate two standard errors. Negative values of b_{ONAP} are not shown.

Conversely, modeled b_{ONAP} values for May 2000 samples were negative at all wavelengths. Modeled regional averages of mass-specific absorption and scattering coefficients of ONAP at selected wavelengths and for May 2000 and April 2001 oceanographic cruises are summarized in Table 2. Similar to lab results, the magnitude of $b_{ONAP}^*(550)$ (up to $0.72 \pm 1.61 \text{ m}^2 \text{ g}^{-1}$) was higher with respect to $a_{ONAP}^*(550)$ (up to $0.50 \pm 0.37 \text{ m}^2 \text{ g}^{-1}$). However, a major difference was observed in the blue spectral region where the mean particulate absorption efficiency per unit of mass was up to 2-fold higher with respect to that corresponding to particulate scattering efficiencies.

Table 2. Modeled mass-specific absorption and scattering coefficients of ONAP based on *in situ* measurements. Between parentheses ± 2 standard errors.

Cruise	λ (nm)	λ (nm)	
		a_{ONAP}^*	b_{ONAP}^*
May 2000	412	2.53 (1.44)	
	550	0.39 (0.29)	
	676	0.025 (0.56)	
April 2001	412	2.44 (1.33)	1.44 (0.87)
	550	0.50 (0.37)	0.72 (0.82)
	676	0.099 (0.30)	1.83 (0.73)

1.6. DISCUSSION

1.6.1. Phytodetritus preparation

The production of organic detritus from phytoplankton cultures was more efficient (i.e., a larger proportion of detritus generated per unit of time) when freezing/thaw and sonication treatments were applied to DT-derived samples. This is reasonable since diatoms have a

silica structure that makes their cells more resistant to breakage. In this study, lab experiments were done with the same phytoplankton genres (e.g., *Thalassiosira sp.*, *Dunaliella sp.*) used by other studies (Biddanda and Pomeroy, 1988; Bidle and Azam, 2001). However, the phytodetritus created in this study is expected to have different characteristics in terms of optical properties, chemical composition and PSD due to methodological differences (e.g., number of cell breakage treatments per day, use of alternative cell disruption techniques such as thermal shock at 55°C) (Biddanda and Pomeroy, 1988; Bidle and Azam, 2001). Here, the sonication of samples not only favored the destruction of cells but also inhibited the formation of aggregates, a well-known process occurring after the bacterial colonization of phytodetritus (Biddanda and Pomeroy, 1988). Thus, our phytoplankton-derived ONAP is anticipated to have a greater fraction of small-sized particles than the same sample without being exposed to ultrasound vibrations.

Differences on cell breakage techniques also determine the time necessary for obtaining chlorophyll-free particulates. The complete degradation of chlorophyll a in this study (i.e., sample fluorescence not different from blank) was obtained after two weeks of cell lysis experiments. Conversely, this pigment degradation state was achieved by Verity et al. (2000) in a longer span (~35 days) due to the lack of freeze/thaw or sonication effects.

In this study, the contamination of phytodetritus by non-native heterotrophic bacteria (i.e., microbial flora incorporated from external sources such as the sonication probe) and subsequent impact on ONAP optical properties was minor. The densities of heterotrophic bacteria were within the range reported by other lab studies focused on phytodetritus (5.5×10^5 to 10^7 cells ml⁻¹) (Biddanda and Pomeroy, 1988). Likewise, the optical contribution of heterotrophic bacteria to the scattering coefficients in our cultures was comparable to that calculated in oceanic waters for native microbial assemblages (Montes-Hugo et al., 2009). Heterotrophic bacteria have no pigments, thus their influence on ONAP optics is mainly attributed to changes on light scattering (Stramski and Kiefer, 1990). The contribution of

non-pigmented bacteria to their beam attenuation coefficient is negligible (< 1%) and mainly occurring in the blue range due to the presence of cytochromes (Stramski and Kiefer, 1998). Unfortunately, no concurrent microbiological and optical data exist in the SLE for computing the relative importance of heterotrophic bacteria to ONAP optical coefficients in samples obtained *in situ*.

1.6.1. Lab-derived optical properties of phytodetritus

Spectrally-normalized curves of phytodetritus absorption coefficient showed a general inverse relationship with respect to wavelength and within the visible-near IR spectral. This general variation was not monotonic due to the existence of shoulders (e.g., $\lambda = 440$ and 555 nm in TP-derived detritus, Fig. 4a). The increase of detritus absorption at shorter wavelengths has been already demonstrated by several studies working in oceanic (Iturriaga and Siegel, 1989; Sosik and Mitchell, 1995) and coastal waters (Babin et al. 2003; Röttgers et al., 2014). Also, the presence of absorption ‘shoulders’ have been previously identified in spectral curves of a_{NAP} and associated to breakdown products of photosynthetic pigments (Iturriaga and Siegel, 1989; Bricaud and Stramski, 1990). Lastly, the flattening of spectral-normalized scattering coefficients of DT- with respect to TP-derived detritus could be attributed to the absence of biogenic minerals in ONAP particles originated from DT samples. In nearshore waters of California, spectral curves of b_p^* showed that organic-rich particle assemblages were characterized by smaller slopes with respect to mineral-dominated particulates (Wozniak et al., 2010).

An important result of this study was the calculation of mass-specific absorption and scattering coefficients of different kinds of phytodetritus. This information did not include particulates smaller than $0.7\text{ }\mu\text{m}$, thus the mass-specific optical measurements made here may not reflect the whole spectrum of ONAP particles at the submicron scale. Also, these estimates are not including optical variations due to aggregates as samples were perturbed by ultrasound and shear before the ac-9 determinations. In this study, the absorption and

scattering efficiency of phytodetritus was not substantially influenced by phytoplankton composition. However, spectral a_{ONAP}^* values of DT- tended to be higher than those corresponding to TP-derived samples. The larger magnitude of a_{ONAP}^* in detritus derived from flagellate cells was likely explained by the lower cellular apparent density (ρ) (i.e., density of organic matter in hydration) of DT- compared to TP-based detritus.

Although the water content of organic detritus or live cells during the experiment was unknown, it is possible to estimate the impact of biogeochemical composition of TP and DT living cells on ρ changes of detrital particles. This analysis assumes that density of living phytoplankton cells and their phytodetritus are comparable. Proteins are the dominant organic component of these phytoplankton species and represent a larger proportion in TP (34%) with respect to DT (20%) cells (Brown, 1991). Also, proteins are relatively heavy ($\sim 1.35 \text{ Kg L}^{-1}$) with respect to lipids ($\sim 0.95 \text{ Kg L}^{-1}$) (Zhang et al., 2014), the second most important organic component of cells (Brown, 1991). Lastly, TP cells and TP-derived detritus contain opal, a mineral with a relatively high density (i.e., $\sim 2.05 \text{ Kg L}^{-1}$) (Twardowski et al., 2001; Zhang et al., 2014). Although plausible, the above interpretation about taxa-related a_{ONAP}^* changes due ρ should be applied with caution since more studies are needed to corroborate this hypothesis.

The magnitude of a_{ONAP}^* of both types of phytodetritus (e.g., $0.066\text{-}0.090 \text{ m}^2 \text{ g}^{-1}$, $\lambda = 443 \text{ nm}$) was in the upper range of values reported for field determinations of a_{NAP}^* in coastal waters ($0.024\text{-}0.041 \text{ m}^2 \text{ g}^{-1}$) (Bowers et al., 1996; Babin et al., 2003). These a_{NAP}^* estimates correspond to European coastal waters and were obtained by linear regression of NAP absorption coefficients as a function of suspended particulate matter concentration measurements. By considering the error around the regression line (coefficient of variation = 56%), the highest estimates derived from Babin et al. (2003a) were up to $0.10 \text{ m}^2 \text{ g}^{-1}$. Thus, this suggests that other sources of mineral (e.g., sediments) and organic (e.g., zooplankton, macroalgae) detritus not related to phytoplankton appear to reduce the net absorption efficiency of organic detritus when a_{NAP}^* values are compared with samples

only dominated by phytodetritus. Lastly, the spectral shape of a_{ONAP}^* in TP- and DT-derived detritus was characterized by a shoulder centered at a wavelength of 550 nm. This feature resembled the one observed in spectral a_{NAP}^* curves obtained by Babin et al. (2003a) in surface waters of the Mediterranean Sea, and may suggest that phytodetritus is a major component of NAP in these specific marine environments.

1.6.2. Uncertainties of modeled ONAP coefficients for the SLE

Error sources of regionally-weighted a_{ONAP} calculations were related to natural variability of particulate absorption (total and phytoplankton), analytical uncertainties linked to PIM measurements, and errors related to the model applied for estimating optical coefficients of inorganic particulates. In general, the largest source of variability was related to spatial changes on a_p (e.g., up to 70.7% in April 2001, $\lambda = 440$ nm) followed by errors on a_{PIM} estimates (up to 52.5% in May 2000) and variations on a_{ph} (up to 9.7% in May 2000).

The analytical error on a_p was mainly attributed to the incomplete removal of multiple scattering effects during the ac-9 measurements (Mohammadpour et al., 2017). This inaccuracy can be improved in the future by using an integrating sphere (Röttgers et al., 2014). The bias due to a_{PIM} was mainly related to the spectral function ‘brown earth’ that is commonly used in marine optics for modeling optical properties of minerals (Mobley, 1995). Brown earth sediments in suspension were measured by Ahn (1990) and may have major differences with respect to other $a_{PIM}(\lambda)$ curves derived from lab (e.g., up to 75.3% at $\lambda = 440$ nm) or *in situ* (up to 135%) measurements made in coastal waters (Ahn, 1990; Babin et al., 2003b; Babin and Strasmki, 2004; Bowers and Binding, 2006; Snyder et al., 2008).

The major source of bias of b_{ONAP} estimates over the whole SLE was related to the spatial variability of total (i.e., mineral + phytoplankton + ONAP) particulate scattering (e.g., up to 39.2% in April 2001, $\lambda = 550$ nm) followed by b_{PIM} (up to 35.6% in May 2000) and b_{ph} (up to 14.6% in May 2000) uncertainties. The overall bias on b_{ONAP} due to b_p errors can be minimized by performing more accurate b_p estimates using an integrated sphere (Röttgers et al., 2014). Direct measurements of b_p based on volume scattering function (VSF) integrals or angular ratios may provide smaller errors (e.g., up to 12% for angles between 0 and 180° and with respect to Mie theory simulations) than those derived from absorption-attenuation meters. However, these alternative techniques are still experimental (Lee and Lewis, 2003; Li et al., 2012). Another important term contributing to the b_{ONAP} bias was the spectral optical cross section of minerals. Here, the spectral library ‘brown earth’ was applied since no determinations of b_{PIM}^* are available for SLE waters. The spectral scattering curve of ‘brown earth’ is the default b_{PIM}^* curve in radiative transfer simulations (Mobley, 1995) even though may present large differences with respect to other types of inorganic particulates measured *in situ* (e.g., up to 32% difference, $\lambda = 550$ nm) or in lab experiments (up to 30%) (Ahn, 1990; Snyder et al., 2008; Stavn and Richter, 2008).

The uncertainty due to b_{ph} was principally originated from the biogeo-optical model proposed by Gordon and Morel (1983) for estimating particulate scattering as a function of chl. This parameterization assumes that b_p is dominated by phytoplankton contributions which is not true at relatively high concentrations of chl (see below section 4.4). Despite this caveat, this model was not the worst alternative for modeling b_{ph} . Indeed, larger uncertainties on b_{ph} might be expected if calculations are based on assuming cell abundance/chl ratios (Felip and Catalan, 2000) combined with VSF and cell abundance measurements (Vaillancourt et al., 2004).

A final step for calculating regionally-weighted a_{ONAP}^* and b_{ONAP}^* values was the calculation of the mean ONAP concentration over the SLE (i.e., [POM^{ONAP}]). In general, the bias on [POM^{ONAP}] estimates was determined by errors on [POM^{phyto}] values (up to 73.4% of [POM^{ONAP}] in May 2000). In order of importance, [POM^{phyto}] uncertainties were mainly attributed to errors on f1 (i.e., [POC^{phyto}]/chl ratio) (up to 87% in April 2001), followed by f2 (i.e., [POM^{phyto}]/[POC^{phyto}] ratio) (up to 17% in May 2000) and spatial variability of chl (up to 1% in May 2000). Lab measurements and satellite-derived estimates showed that [POC^{phyto}]/chl ratios of phytoplankton cultures decrease with water temperature, increase with photosynthetically available light and decrease at high nutrient concentrations (Geider, 1987; Cloern et al., 1995; Behrenfeld et al., 2002; Behrenfeld et al., 2005).

In our study, the range of [POC^{phyto}]/chl ratios varied between 0.015 and 0.065 based on maximum water temperatures measured in the SLE during summer (up to 18°C), vertically averaged irradiance levels lower than 1 mol photons m⁻² h⁻¹, and non-limiting nutrient conditions for phytoplankton growth. Notice that models of [POC^{phyto}]/chl ratios have never included measurements using dinoflagellates cultures, thus even larger uncertainties on [POC^{phyto}]/chl ratios estimates might be anticipated during blooms of *Alexandrium tamarense* in SLE waters. The uncertainty of f2 was probably underestimated since POM/POC ratios derived from organic detritus may differ from POM/POC ratios derived from phytoplankton cells. To our knowledge, this type of information has never been published and will be an important topic for future investigations.

1.6.3. Optical properties of ONAP in the SLE

In the SLE, optical coefficients of ONAP were modeled using data collected during late and early spring of 2000 and 2001, respectively. In general, May 2000 coincided with a greater river discharge (15.7×10^3 m³ s⁻¹) and weaker wind intensity (6.6 m s⁻¹) with respect to April 2001 (14×10^3 m³ s⁻¹ and 9 m s⁻¹, respectively). However, our spatially-averaged

$a_{ONAP}(440)$ estimates were not substantially different between surveys (mean of two surveys, $0.68 \pm 0.11 \text{ m}^{-1}$, 1 standard deviation). Conversely, the absorption contribution due to minerals was larger during the former period ($a_{PIM}(440) = 0.14$ and 0.11 m^{-1} for May 2000 and April 2001, respectively). This indicates that changes on river flow and associated transport of sediments for these two periods under study have a greater impact on NAP with respect to wind-driven resuspension of particulates. Also, these results suggest that optical properties of organic detritus are more conservative than mineral detritus between the periods under investigation.

In this study, the regional mean of simulated $a_{ONAP}(440)$ during each survey was within the range of $a_{NAP}(440)$ values reported by Xie et al. (2011) for surface waters (i.e., 2 m depth) of the SLE and during May of 2007 (i.e., $0.05\text{-}2.1 \text{ m}^{-1}$). Notice that particulate absorption determinations by Xie et al. (2011) were made following the transmittance-reflectance method (hereafter TR) (Tassan and Ferrari, 2002). In coastal waters of Europe, the magnitude of $a_{NAP}(440)$ as derived from TR measurements may change up to 3 orders of magnitude (0.001 to 1 m^{-1}) (Babin et al., 2003a). Similar to modeled coefficients of ONAP, *in situ* measurements of $a_{NAP}(440)$ during May 2000 ($0.110 \pm 0.034 \text{ m}^{-1}$, 2 standard errors) and April 2001 ($0.147 \pm 0.137 \text{ m}^{-1}$) showed no substantial inter-annual differences even though the magnitude of field determinations was always lower with respect to $a_{ONAP}(440)$ simulations. This is counterintuitive as NAP includes ONAP, thus methodological differences may be likely a major factor explaining inconsistencies between a_{ONAP} and a_{NAP} estimates. *In situ* measurements of a_{NAP} were performed using the pad-technique (Mitchell et al., 2002), thus large errors can be expected in littoral environments such as the SLE due to the high concentration of inorganic particulates (i.e., $> 1 \text{ g m}^{-3}$). Minerals increase the single scattering albedo of samples (i.e., the scattering contribution to the attenuation of light), thus a dominant fraction of photons are reflected and not absorbed by the filter. This effect, if not corrected, leads to a major underestimation of a_{NAP} , thus other more accurate

methods should be applied (e.g., absorption-attenuation meters, integrating sphere, transmission-reflection) (Tassan and Ferrari, 2002; McKee et al., 2013 ; Röttgers et al., 2014).

Calculated scattering coefficients of ONAP for SLE locations and during April 2001 showed minimum values at a wavelength of 555 nm ($0.27 \pm 1.50 \text{ m}^{-1}$). This regional arithmetic mean is close to the averaged b_{POM} value computed for very turbid waters of the Mississippi Delta (0.25 m^{-1}) (Stavn and Richter, 2008). In this case, POM and PIM scattering coefficients were derived from multiple regression case II and using discrete water measurements of organic and inorganic fractions of suspended particulate matter and optical information obtained from ac-9 measurements. Despite this agreement, the spectral shape of b_{ONAP} for April 2001 was quite different to that reported by Stavn and Richter (2008). Indeed, the maximum scattering of POM in coastal waters of the Gulf of Mexico occurred at 550 nm. This spectral variation between SLE and Gulf of Mexico samples was in part attributed to the type of minerals used in this study since the spectral scattering curve for ‘brown earth’ minerals (Ahn, 1990) has a maximum at 550 nm. This conclusion is drawn after computing b_{PIM} with PIM values measured over the SLE and spectral b_{PIM}^* estimates obtained by Stavn and Richter (2008). The spatially-averaged b_{ONAP} estimates for May 2000 were negative due errors related to the selection of the spectral curve of b_{PIM}^* and the limitations of using a case I water model for modeling b_{ph} . The inadequate simulation of optical contribution of minerals to the scattering coefficient was probably not the major factor explaining the large underestimation of b_{ONAP} since negative values were also present after using mass-specific coefficients of PIM derived from coastal waters of the Mississippi Delta (Stavn and Richter, 2008). Based on Gordon and Morel (1983) model, the calculation of phytoplankton contribution to particulate scattering was strongly biased during May 2000 due to the relatively high chl values. As chlorophyll increases, a major fraction of b_p is represented by chl-covarying organic detritus derived from phytoplankton, thus the assumption of negligible scattering effects due to organic detritus is

no longer valid. This explained the positive values of b_{ONAP} during April 2001 due to the lower phytoplankton pigment concentrations ($\text{chl} < 1 \text{ mg m}^{-3}$) and associated small b_{ph} estimates during that period. The uncertainties of Gordon and Morel (1983) model were not related to the choice of B1 since negative estimates were still present after modifying equation (8) with a minimum B1.

The magnitude of b_{ph} can be alternatively estimated by subtracting a_{ph} from the attenuation coefficient of phytoplankton (c_{ph}). Based on empirical measurements in oceanic waters, Voss (1992) found a power-type relationship between c_{ph} and chl at a wavelength of 550 nm:

$$c_{ph}(550) = m1 \text{ chl}^{0.57}, \quad (10)$$

where $m1$ is varying between 0.06 and 0.6 for a given chl value. The spectral curve of c_{ph} is reconstructed based on the empirical expression proposed by Roesler and Boss (2003):

$$c_{ph}(\lambda) = c_{ph}(550) (550/\lambda)^{m2} \quad (11)$$

$$m2 = -0.4 + (1.6 + 1.2 R3)/(1 + \text{chl}^{0.5}) \quad (12)$$

where $m2$ is a random variable between -0.1 and 2 (Sathyendranath et al., 1989) and $R3$ is another random variable that changes between 0 and 1. A sensitivity analysis demonstrated that modeled b_{ONAP} values during May 2000 become positive when $m1$ vary between 0.06 and 0.1. The influence of $m2$ on b_{ONAP} variability was minor (i.e., up to 2%). Assuming an average $m1$ and $m2$ of 0.1 and 0.5, respectively, resulting b_{ONAP} values for May 2000 within the visible-near-IR spectral range were up to 1 order of magnitude lower (e.g., $b_{ONAP}(550) = 0.045 \pm 2.66 \text{ m}^{-1}$) with respect to April 2001 ($b_{ONAP}(550) = 0.45 \pm 2.32 \text{ m}^{-1}$) values. This is consistent with the greater mineral-enrichment of surface waters of the SLE during spring of 2000. Thus, the new calculation of b_{ph} provided a better closure for estimating b_{ONAP} in our samples than the original model presented in equation (8).

Unlike $a_{ONAP}(\lambda)/a_{ONAP}(412)$ curves, the variation of spectrally-normalized b_{ONAP} estimates showed a clear difference between surveys. This additional analysis based on equations (10-12) suggests that b_{ONAP} estimates during April 2001 were less spectrally dependent than those computed for May 2000. This spectral flattening in spring 2001 samples coincided with a relatively low trophic status and a phytoplankton community dominated by flagellates. This is consistent with our lab results since phytodetritus derived from DT cells (i.e., microflagellates) was characterized by a less variable $b_{ONAP}(\lambda)/b_{ONAP}(412)$ spectrum with respect that originated from TP cells (i.e., diatoms). The spatially-weighted arithmetic average of a_{ONAP}^* over the SLE was comparable between surveys (e.g., $a_{ONAP}^*(440) = 1.67 \pm 1.22$ and $1.61 \pm 1.05 \text{ m}^2 \text{ g}^{-1}$ for May 2000 and April 2001, respectively). To our knowledge, no simulations or measurements of $a_{ONAP}^*(440)$ have been cited in the literature. Thus, the validity of these results was verified indirectly by comparing our calculations of a_{POM}^* with estimates derived from other studies. Calculated values of a_{POM}^* in the SLE (e.g., 0.99 ± 0.91 and $1.47 \pm 0.97 \text{ m}^2 \text{ g}^{-1}$ for May 2000 and April 2001, respectively, $\lambda = 440 \text{ nm}$) were within the range of absorption cross sections of POM reported in turbid near-shore waters of US by Snyder et al. (2008) (e.g., $0.20\text{-}0.70 \text{ m}^2 \text{ g}^{-1}$). Notice that optical cross sections derived from Snyder et al. (2008) were obtained based on multiple regression analysis. Similar to a_{ONAP}^* , there are not references in the literature to corroborate the magnitude of our b_{ONAP}^* calculations. The mass-specific scattering coefficient of POM in the SLE (e.g., 0.33 ± 1.45 and $1.24 \pm 1.52 \text{ m}^2 \text{ g}^{-1}$ for May 2000 and April 2001, respectively, $\lambda = 550 \text{ nm}$) was within the range of optical cross sections ($0.67\text{-}1.25 \text{ m}^2 \text{ g}^{-1}$) calculated by Stavn and Richter (2008) in coastal waters of US.

1.7. CONCLUSIONS

In this study, controlled lab experiments were performed for producing phytodetritus and measuring their inherent optical characteristics. Also, the magnitude and spectral behavior

of absorption and scattering coefficients of phytodetritus were compared with a_{NAP} and b_{NAP} measurements reported in coastal waters and simulated optical coefficients of ONAP derived from samples obtained in the SLE during spring. Our lab results suggest that optical coefficients of phytodetritus have large uncertainties that preclude any clear taxonomic differentiation. However, two trends were observed where detritus derived from flagellate cells tended to have higher mass-normalized absorption coefficients and flatter spectral curves of scattering coefficients than detritus originated from diatoms. These apparent differences were related to differences in apparent density of ONAP particles and the presence/absence of biogenic silicate, respectively. Mass-specific absorption coefficients of phytodetritus corrected by bacteria contamination were within the upper range of a_{NAP}^* values reported in coastal waters and suggest that phytoplankton-based detritus is probably characterized by higher absorption efficiencies per unit of mass with respect to those coefficients associated to mineral or non-living organic particles derived from non-phytoplankton sources.

The main challenges in calculating regional optical coefficients of ONAP in SLE waters were related to the analytical error of particulate absorption measurements, the lack of local information regarding the optical properties of inorganic particulates, and uncertainties associated to the quantification of phytoplankton contribution to POM. Despite these limitations, the following patterns were identified: 1) regional-weighted absorption coefficients of $a_{ONAP}(440)$ during spring did not have substantial changes between years as suggested by 2000-2001 surveys, 2) the modeling of b_{ph} based on equations (10-12) suggest a higher regional mean of $b_{ONAP}(550)$ during April 2001 that was attributed to a lower optical contribution of mineral particulates and phytoplankton to b_p with respect to May 2000, and 3) the shape of simulated $b_{ONAP}(\lambda)$ spectrum appeared to indicate phytoplankton communities changes between May 2000 and April 2001 surveys.

CONCLUSION GÉNÉRALE

À travers cette étude on a pu définir les caractéristiques optiques des particules non-algales organiques origines de cultures de phytoplancton et des modèles développés avec des données collectées dans l'ESL.

Initialement, l'objectif principal du projet était d'étudier les propriétés optiques des détritus organiques issus de deux espèces de phytoplancton mises en culture. Au fur et à mesure de l'avancement du projet, il s'est avéré nécessaire d'ajouter une deuxième section incluant des données du terrain afin de comparer les détritus de différentes origines.

En premier lieu, un protocole de production des détritus organiques combinant deux types de traitement (congélation/décongélation et sonification) a été mis au point. Le développement de cette méthodologie a été d'une grande importance pour l'étude des signatures des phytodétritus, l'un des groupes faisant partie des particules non algales organiques dans les eaux océaniques et littorales. L'alternance entre les deux procédés a permis une destruction effective des cellules phytoplanctoniques étudiées.

En deuxième lieu, une estimation de la biomasse bactérienne avant et après chaque mesure optique a été faite. Elle a permis d'éliminer la contribution bactéries hétérotropiques aux IOPs des phytodétritus, qui s'est avérée comparable à celle des milieux océaniques. La distribution des classes de tailles de ces particules a été nécessaire pour l'interprétation des IOPs des phytodétritus issus de deux différentes espèces de phytoplancton.

En troisième lieu, une caractérisation des propriétés optiques des phytodétritus a pu être effectuée, offrant ainsi une analyse de la diffusion et de l'absorption de la lumière par ces

particules. Les deux espèces de phytoplancton étudiées, ont été discriminées sur la base d'hypothèses liées à l'influence de la composition chimique des ONAP sur leur comportement optique. En effet, le coefficient de diffusion des ONAP, normalisé, issus de TP, montre une plus grande diffusion dans les courtes longueurs d'ondes en raison de la présence de silice biogénique.

Dans le deuxième volet, les résultats préliminaires obtenus grâce aux IOPs modélisées au niveau de l'Estuaire du St-Laurent, suggèrent que les ONAP au niveau de l'Estuaire du Saint-Laurent ont un coefficient d'absorption spécifique à la masse plus élevé que celui des particules non algales inorganiques. Les données du terrain ont également révélé des variations interannuelles importantes liées aux changements de la diffusion totale des particules due aux minéraux. Quant aux changements spectraux des moyennes régionales de b_{ONAP} , ils étaient liés aux larges modifications des communautés phytoplanctoniques dominantes dans le SLE.

Limites et perspectives :

Pendant le déroulement de ce projet, plusieurs problèmes ont été rencontrés limitant ainsi le champ d'étude et objectifs ciblés. Ces problèmes pourraient être évités en améliorant les différents protocoles suivis. Concernant la production des détritus organiques, il n'a pas été facile de garder les échantillons dans un état axénique en raison de l'environnement de travail. L'utilisation d'un type de sonicateur autre que le sonicateur à tige (exemple : bain à ultrasons) est préférable, car il ne nécessite pas un contact entre l'échantillon et l'air. Il serait également plus prudent d'effectuer les mesures sous une hotte à flux laminaire afin d'éviter la contamination par des particules en suspension dans l'air.

Des suggestions pour des études futures, basées sur les résultats obtenus grâce à ce projet pourraient être regroupées comme suit :

- Choix d'un nombre d'espèces phytoplanctoniques plus élevé, toutes différentes en termes de composition chimique, taille et forme.
- Caractérisation des propriétés optiques et chimiques des cellules phytoplanctoniques avant et après destruction de leurs parois cellulaires. Ceci permettrait de construire une base de données sur les différents groupements chimiques qui sont présents dans ces cellules. Cette base servira pour l'analyse de la variation de la composition chimique suite aux traitements mais aussi d'étudier l'effet de la variation des IOPs des particules en fonction de leur nature chimique.

Finalement, les objectifs atteints par cette étude représentent un pas vers l'analyse et la compréhension du comportement optique des ONAP et leur contribution à la variation du signal satellitaire. Leur rôle dans la variation des IOPs des milieux marins a été mieux défini par, ce qui ouvre la porte à des études futures, plus précises et plus approfondies sur l'origine des signaux en télédétection optique.

RÉFÉRENCES BIBLIOGRAPHIQUES

- Aas, E. 1996. Refractive index of phytoplankton derived from its metabolite composition. *Journal of Plankton Research*, Volume 18, Issue 12, 1 December 1996, Pages 2223–2249.
- Ahn, Y.H. 1990. Propriétés optiques des particules biologiques et minérales présentes dans l'océan. Thèse, Université Pierre et Marie Curie, pp. 208.
- Anesio, A.M., Aabreu, P.C. et Biddanda, B.A. 2003. The role of free and attached microorganisms in the decomposition of estuarine macrophyte detritus. *Estuar. Coast. Shelf Sci*, 56, 197-201.
- Annane, S., Starr, M., Pelletier, E. et Ferreyra, G. 2015. Contribution of exopolymeric particles (TEP) to estuarine particulate organic carbon pool. *Mar. Ecol. Progr. Ser.*, 529, 17-34.
- Babin, M., Therriault, J.C., Legendre, L. et Condal, A. 1993. Variations in the specific absorption coefficient for natural phytoplankton assemblages: Impact on estimates of primary production. *Limnol Oceanogr* 38(1): 154-177.
- Babin, M., Morel, A., Fournier-Sicre, V., Fell, F. et Stramski, D. 2003. Light scattering properties of marine particles in coastal and open ocean waters as related to the particle mass concentration. *Limnol. Oceanogr. Methods*, 48, 843–85.
- Babin, M. et Stramski, D. 2004. Variations in the mass-specific absorption coefficient of mineral particles suspended in water. *Limnol. Oceanogr.*, 49, 756-767.
- Balch, W.M. 2000. Light scattering by viral suspensions. *Limnol Oceanogr* 45(2), 492-498.
- Baker, MJ., Trevisan, J., Bassan, P., Bhargava, R., Butler, HJ., Dorling, K.M., Martin, F.L. 2014. Using Fourier transform IR spectroscopy to analyze biological materials. *Nature protocols*, 9, 1771-1791.

- Barillé-Boyer, A.L., Barillé, L., Massé, H., Razet, D. et Héral, M. 2003. Correction for particulate organic matter as estimated by loss on ignition in estuarine ecosystems. *Estuar. Coast. Shelf Sci.*, 58, 147–153
- Bauerfeind, S. 1985. Degradation of phytoplankton detritus by bacteria: estimation of bacterial consumption and respiration in an oxygen chamber. *Mar. Ecolog. Progress. Series*, 21, 27-36.
- Behrenfeld, M. J., Marañon, J.E., Siegel, D.A. et Hooker, S.B. 2002. A photoacclimation and nutrient based model of light-saturated photosynthesis for quantifying oceanic primary production, *Mar. Ecol. Prog. Ser.*, 228, 103– 117.
- Behrenfeld, M.J., Boss, E., Siegel, D.A. et Shea, D.A. 2005. Carbon-based ocean productivity and phytoplankton physiology from space. *Glob. Biogeoch. Cycles*, 19, GB1006, doi:10.1029/2004GB002299.
- Biddanda, B.A., Pomeroy, et L.R. 1988. Microbial aggregation and degradation of phytoplankton-derived detritus in seawater. 1 Microbial succession. *Mar. Ecol. Progr. Ser.*, 42, 79-88.
- Bidle, K.D. et Azam, F. 2001. Bacterial control of silicon regeneration from diatom detritus: Significance of bacterial ecotohydrolases and species identity. *Limnol. Oceanogr.*, 46, 1606-1623.
- Bowers, D.G. et Binding, C.E. 2006. The optical properties of mineral suspended particles: A review and synthesis, *Estuar. Coast. Shelf Sci.*, 67, 219–230.
- Bowers, D.G., Harker, G.E.L. et Stephan, B. 1996. Absorption spectra of inorganic particles in the Irish Sea and their relevance to remote sensing. *Int. J. Rem. Sens.*, 17, 2449-2460.
- Boyd, P.W., Sherrya, N.D., Berge, J.A., Bishop, J.K.B., Calverta, S.E., Charette, M.A.,, Wong, C.S. 1999. Transformations of biogenic particulates from the pelagic to the deep ocean realm. *Deep Sea Res., II* 46, 2761-2792.
- Bricaud, A. et Morel, A. 1986. Light attenuation and scattering by phytoplanktonic cell s: A theoretical modeling. *Appl Opt* 25:571-580

- Bricaud, A. et Stramski, D. 1990. Spectral absorption coefficients of living phytoplankton and non-algal biogenous matter: a comparison between the Peru upwelling and the Sargasso Sea. Limnol. Oceanogr., 35, 562-582.
- Brown, M.R. 1991. The amino acid and sugar composition of 16 species of microalgae used in mariculture. Aquaculture, 145, 79-99.
- Brunns, E.A., Perraud, V., Zelenyuk, A., Ezell, M.A., Johnson, S.N., Yu, Y., ... Alexander, M.L. 2010. Comparison of FTIR and Particle Mass Spectrometry for the Measurement of Particulate Organic Nitrates. Environ. Sci. Technol., 44, 1056–1061.
- Cael, B.B. et Boss, E. 2017. A simplified model of spectral absorption by non-algal particles and dissolved organic materials in aquatic environments. Opt. Expr., 25, 25486-25491.
- Carder, K.L., Steward, R.G., Harvey, G.R. et Ortner, P.B. 1989. Marine humic and fulvic acids: Their effects on remote sensing of ocean chlorophyll, Limnol. Oceanogr., (341):68–81.
- Cermak, N., Becker, J.W., Knudsen, J.M., Chisholm, S.W., Manalis, S.R. et Polz, M.F. (2016). Direct single-cell biomass estimates for marine bacteria via Archimedes' principle. ISME, 1-4. 1751-7362/16
- Cloern, J. E., Grenz, C. et Vidergar-Lucas, C. 1995. An empirical model of the phytoplankton chlorophyll/carbon ratio: The conversion factor between productivity and growth rate, Limnol. Oceanogr, 40, 1313 –1321.
- D'Anglejan, B.F., Smith, E.C. 1973. Distribution, transport and composition of suspended matter in the St. Lawrence Estuary. Can. J. Earth Sci., 10, 1380-1396.
- Demaster, D.J. 2003. The diagenesis of biogenic silica: chemical transformations occurring in the water column, seabed and crust. In: Holland H.D., Turekian K.K. (eds). Treatise in Geochemistry, vol. 7, Pergamon, Oxford, pp. 87-98.
- Dunne, J.P., Amstrong, R.A., Gnadasikan, A., et Sarmiento, J.L. 2005. Empirical and mechanistic models for the particle export ratio. Glob. Biogeochem. Cycles, 19, doi: 10.1029/2004GB002390.

- DuRand, M.D. et Olson, R.J. 1998. Diel patterns in optical properties of the chlorophyte *Nannochloris* sp.: relating individual-cell bulk measurements. *Limnol. Oceanogr.*, 43, 1107-1118.
- El-Sabh, M.I. 1979. The lower St. Lawrence estuary as a physical oceanographic system. *Naturalist Canadian*, 106, 55-73.
- El-Sabh, M.I. et Silverberg, N. 1992. The St. Lawrence Estuary: Introduction. In *Oceanography of a Large-Scale Estuarine System*. Edited by M.I. El-Sabh and N. Silverberg. Springer-Verlag, pp. 1-9.
- Eyre, B.D., Maher, D.T. et Squire, P. 2013. Quantity and quality of organic matter (detritus) drives Neffluxes (net denitrification) across seasons, benthic habitats, and estuaries. *Global Biogeochem. Cycles*, 27, 1083–1095.
- Felip, M. et Catalan, J. 2000. The relationship between phytoplankton biovolume and chlorophyll in a deep oligotrophic lake: decoupling in their spatial and temporal maxima. *J. Plank. Res.*, 22, 91-105.
- Gardner, W.D., Walsh, I.D. et Richardson, M. 1993. Biophysical forcing of particle production and distribution during a spring bloom in the North Atlantic. *Deep-Sea Res II*, 40: 171-195.
- Geider, R.J. 1987. Light and temperature dependence of the carbon to chlorophyll ratio in microalgae and cyanobacteria: Implications for physiology and growth of phytoplankton, *New Phytol.*, 106, 1 –34.
- Gilerson, A., Zhou, J., Oo, M., Chowdhary, J., Gross, B.M., Moshary, F. et Ahmed S. 2006. Retrieval of chlorophyll fluorescence from reflectance spectra through polarization discrimination: Modeling and experiments. *Applied Optics*, 45, 5568-5581.
- Gobeil, C., Sundby, B., et Silverberg, N. 1981. Factors influencing particulate matter geochemistry in the St. Lawrence estuary turbidity maximum. *Marine Chemistry*, 10:123–140.
- Gohin, F. 2011. Annual cycles of chlorophyll-a, non-algal suspended particulate matter, and turbidity observed from space and in-situ in coastal waters. *Ocean Sci.*, 7, 705-732.

- Gordon, H.R., Brown, O.B., Evans, R.H., Brown, J.W., Smith, R.C., Baker, K.S., Clark, D.K. 1988. A semianalytic radiance model of ocean color. *J Geophys Res* 93: 10909-10924
- Gordon, H.R., Brown, O.B. et Jacobs M.M., 1975. Computed relationships between the inherent and apparent optical properties of a fiat homogeneous ocean. *Appl Opt.*, 14, :417-427.
- Gordon, H. R., et A. Morel, Remote assessment of ocean color for interpretation of satellite visible imagery: A review, 114 pp., Springer-Verlag, New York, 1983.
- Gordon, H.R., Smyth, T.J., Balch, W.M., Boynton, G.C. et Tarran, G.A. 2009. Light scattering by coccoliths detached from *Emiliania huxleyi*. *App. Opt.*, 48, 6059-6073.
- Green, R.E., Gould, R.W. et Ko, D.S. 2008. Statistical models for sediment/detritus and dissolved absorption coefficients in coastal waters of the northern Gulf of Mexico. *Cont. Shelf Res.*, 28, 1273-1285.
- Green, R.E., Sosik, H.M., et Olson, R.J. 2003. Contributions of phytoplankton and other particles to inherent optical properties in New England continental shelf waters. *Limnol. Oceanogr.* 48, 2377–2391
- Groundwater, H., Twardowski, M., Dierssen, H., Sciandra, A. et Freeman, S.A., 2012 Determining Size Distributions and Composition of Particles Suspended in Water: A New SEM–EDS Protocol with Validation and Comparison to Other Methods. *J. Atm. And Ocean. Tech.*, 29, 433-449.
- Hamilton, S.K., Sippel, S.K. et Bunn, S.E. 2005. Separation of algae from detritus for stable isotope or ecological stoichiometry studies using density fractionation in colloidal silica. *Limnol. Oceanogr. Methods* 3, 149-157.
- Higgs, N.D., Gates, A.R. et Jones, D.O.B. 2014. Fish food in the deep sea: revisiting the role of large food-falls. *PloS one*, 9,e96016.: doi:10.1371/journal.pone.0096016.
- Hoge, F.E., Wright, C.W., Swift, R.N., Yunge, J.K., Berry, R.E. et Mitchell, R. 1998. Airborne biooptics survey of the Galapagos Islands margins. *Deep-Sea Res* 1145: 1083-1092. 40(2):411-41.

- Iturriaga, R. et Siegel, D. A. 1989. Microphotometric characterization of phytoplankton and detrital absorption properties in the Sargasso Sea, Limnol. Oceanogr., 34, 1706–1726.
- Karlson, A.M.L., Niemand, C., Savahe, C. et Pilditch, C.A. 2016. Density of key-species determines efficiency of macroalgae-detritus uptake by intertidal benthic communities. PloS one, 11, e0158785, doi: 10.1371/journal.pone.0158785.
- Kelaher, B., Bishop, M.J., Potts, J., Scanes, P. et Skilbeck, G. 2013. Detrital diversity influence estuarine ecosystem performance. Global Change Biol., 19, 1909–1918.
- Kishino, M.N., Takahashi, N., Okami, N. et Ichimura, S. 1985. Estimation of the spectral absorption coefficients of phytoplankton in the sea. Bull. Mar. Sci. 37, 634-642.
- Kitchen, J. C. et Zaneveld, J. R. V. 1992. A three-layered sphere model of the optical properties of phytoplankton. Limnol. and Oceanogr., 37, 1680–1690.
- Lam, P.J., Ohnemus, D. et Auto, M.E. 2015. Size-fractionated major particle composition and concentrations From the US GEOTRACES North Atlantic Zonal Transect. Deep Sea Res. II, 116, 303-320.
- Larouche, P. et Boyer-Villemaire, U., 2010. Suspended particulate matter in the St. Lawrence estuary and Gulf surface layer and development of a remote sensing algorithm. Estuarine, Coastal and Shelf Science 90, 241–249. doi:10.1016/j.ecss.2010.09.005
- Lee, M.E. et Lewis, M.R. 2003. A new method for measurement of the optical volume scattering functionin the upper ocean. American Meteorological Society, 20,563-571.
- Lee, Z. et Hu, C. 2006. Global distribution of case I waters: Aan analysis from SeaWiFS measurements. Rem. Sens., 101, 270-276.
- Li, C., Cao, W., Yu, J., KE,t., Lu, G.,Yang,Y. et Guo, C. 2012. An instrument for in situ measuring the volume scattering function of water: Design, calibration and primary experiments. Sensors, 12, 4514-4533.

- Loisel, H. et Morel, A. 1998. Light scattering and chlorophyll concentration in case 1 waters: A reexamination. *Limnol Oceanogr* 43(5):847-858.
- Loisel, H., Duforet, L., Dessailly,D., Chami, M., et Dubuisson, P. 2008. Investigation of the variations in the water leaving polarized reflectance from the POLDER satellite data over two biogeochemical contrasted oceanic areas. *Opt. expr.*, 17, 12905-12918.
- Maritorena, S., Siegel, D. A. et O'Reilly, J. E. 2004. Optical properties of oceanic Case 1 waters: Still an issue!! American Society of Limnology and Oceanography/The Oceanography Society, Ocean Research 2004 Conference, Honolulu, February 2004.
- McKee, D., Piskozub, J. et Brown, I.. 2008. Scattering error corrections for in situ absorption and attenuation measurements. *Opt. Exp.*, 16, 19480-19492.
- McKee, D., Piskozub, J., Röttgers, R. et Reynolds, R.A. 2013. Evaluation and improvement of an iterative scattering correction scheme for in situ absorption and attenuation measurements, *J.Amer. Ocean. Technol.*,30, doi.10.1175/JTECH-D-12-00150.1.
- McKee, D.J.C. et Chami, M. 2007. Determination of biogeochemical properties of marine particles using above water measurements of the degree of polarization at the Brewster angle. *Optics Express*, 15, 9494-9509.
- Melack, J.M. 1985. Interactions of detrital particulates and plankton. *Hydrobiologia.*, 125, 209-220.
- Menzel, D.W. et Goering, J.J. 1966. The distribution of organic detritus in the ocean. *Limnol. Oceangr.*, 11, 333-337.
- Mitchell, B.G., Kahru, M., Wieland, J. et Stramska, M. 2002. Determination of spectral absorption coefficients of particles, dissolved material and phytoplankton for discrete water samples, in *Ocean Optics Protocols for Satellite Ocean Color Sensor Validation*, Rev. 4, Vol. IV: Inherent Optical Properties: Instruments, Characterizations, Field Measurements and Data Analysis Protocols, J. L. Mueller, G. S. Fargion, and C. R. McClain, eds. (NASA Goddard Space Flight Center, NASA/TM-2003-211621/Rev4-Vol. IV, 2003, 39-64.

- Mobley, C.D. 1994. Light and water: radiative transfer in natural waters. Academic Press Inc, London, 592 pp.
- Mobley, C.D. 1995. Hydrolight 3.0 User's Guide, SRI International, Menlo Park, Calif.1995.
- Mobley, C.D., Sundman L. K. et Boss, E. 2002. Phase function effects on oceanic light fields. *Appl. Optics* 41: 10351050, doi:10.1364/AO.41.001035
- Mobley, C.D. 1999. Estimation of the remote-sensing reflectance from above-surface measurements. *Appl Opt*, 38(36): 7442–7455
- Mohammadpour, G., Gagné, J.P., Larouche, L. et Montes-Hugo, M.A. 2017. Optical properties of size fractions of suspended particulate matter in littoral waters of Quebec. *Biogeosciences*, 14, 1-16.
- Mohammadpour, G., Gagne, J.P., Larouche, P. et Montes-Hugo, M. 2015. Particle Composition Effects on MERIS-derived SPM: A Case Study in the Saint Lawrence Estuary. *Can. J. Rem. Sen.*, 41, 515-524.
- Montes-Hugo, M. A., Reynolds, R. A., Vernet, M.; Stramski, D. et Wright, V. 2007. Particulate beam attenuation coefficient, bacteria abundance, and production in marine nearshore waters. *SPIE 2007SPIE.6680E..17M*.
- Montes-Hugo M. et Xie, X. 2015. An inversion model based on salinity and remote sensing reflectance for estimating the phytoplankton absorption coefficient in the SaintLawrence Estuary. *J Geoph Res*, doi.10.1002/2015jc011079.
- Montes-Hugo, M., Ducklow, H., et Schofield, O.M. 2009. Contribution by different marine bacterial communities to particulate beam attenuation. *Mar. Ecol. Progr. Ser.*, 379, 13-22.
- Montes-Hugo, M.A., Roy, S., Gagne, J.P., Demers, S., Cizmeli, S. et Mas, S. 2012. Ocean colour and distribution of suspended particulates in the St. Lawrence estuary. *EARSEL eProc.*, 11, 1–11.
- Montes-Hugo, M.A., Roy, S., Gagne, J.P., Demers, S., Cizmeli, S. et Mas, S. 2012. Ocean colour and distribution of suspended particulates in the St. Lawrence estuary. *EARSeL eProc.*, 11, 1–11.

- Morel, A. et Prieur L.1977. Analysis of variations in ocean color. Limnol. Oceanogr., 22(4),: 709-722.
- Morel, A. et Gentili, B. 1991. Diffuse reflectance of oceanic waters: its dependence on sun angle as influence by molecular scattering contribution. Appl Opt 30:4427-4438.
- Morel, A. 1974. Optical properties of pure water and pure sea water, in Optical aspects of oceanography, edited by N.G. Jerlov, and Nielsen, E.S., pp. 1-24, Academic, New York, 1974.
- Morel, A. et Bricaud, A. 1986. Inherent optical properties of algal cells including picoplankton: Theoretical and experimental results, p. 521–559. In T. Platt and W. K. W. Li [eds.], Photosynthetic picoplankton. Can. Bull. Fish. Aquat. Sci. 214.
- Mostajir, B., Dolan, J.R. et Rassoulzadegan, F. 1995. Seasonal variations of pico- and nano-detrital particles (DAPI Yellow Particles, DYP) in the Ligurian Sea (NW Mediterranean). Mar. Ecol. Progres. Ser., 9, 267-277.
- Nelson, J.R. 1993. Rates and possible mechanism of light-dependent degradation of pigments in detritus derived from phytoplankton. J. Mar. Syst., 51, 155-179.
- Nelson, J.R. et Robertson, C.Y. 1993. Detrital spectral absorption: Laboratory studies of visible light effects on phytodetritus absorption, bacterial spectral signal, and comparison to field measurements. J. Mar. Syst., 51, 181-207.
- Nelson, N.B., Siegel, D.A., Carlson, C.A., Swan, C., Smethie, W.M. Jr. et Khatiwala, S., 2007, 454 Hydrography of chromophoric dissolved organic matter in the North Atlantic, Deep Sea Research Part 1, 54, 710-731.
- Nelson, N.B., Siegel, D.A. et Michaels, A.F., 1998, Seasonal dynamics of colored dissolved 450 material in the Sargasso Sea, Deep Sea Research Part 1, 45, 931-957.
- Neukermans, G., Loisel, H., Mériaux, X., Astoreca, R. et McKee, D. 2012. In situ variability of mass-specific beam attenuation and backscattering of marine particles with respect to particle size, density, and composition, Limnol. Oceanogr., 57, 124–144.

- Nieke, B., Reuter, R., Heuermann, R., Wang, H., Babin, M. et Therriault, J.C., 1997. Light absorption and fluorescence properties of chromophoric dissolved organic matter (CDOM) in the St. Lawrence Estuary (Case 2 waters). *Cont. Shelf Res.*, 17, 235–252
- Nixon, S.W., Fulweiler, R.W., Buckley, B.A., Granger, S.L., Nowicki, B.L. et Henry, K.M. 2009. The impact of changing climate on phenology, productivity and benthic-pelagic coupling in Narragansett Bay, *Estuarine Coastal Shelf Sci.*, 82, 1–18.
- O'Reilly, J.E., Maritorena, S., Mitchell, B.G., Siegel, D.A., Carder, K.L., Garver, S.A. et McClain, C.R. 1998. Ocean color chlorophyll algorithms for SeaWiFS . *J Geophys Res* 103:24937-24953.
- Oliver, R.L., Kinnear, A.J. et Ganf, G.G. 1981. Measurements of cell density of three freshwater phytoplankters by density gradient centrifugation. *Limnol. Oceangr.*, 26, 285-294.
- Pegau, S., Gray, D. et Zanaveld, J.R.V. 1997. Absorption and attenuation of visible and near-infrared light in water: Dependence on temperature and salinity. *Appl. Opt.* 36, 6035–6046.
- Platt, T., Harrison, W.G., Lewis, M.R., Li, W.K.W., Sathyendranath, S., Smith, R.E. et Vézina, A.F. 1989. Biological production of the oceans: the case for a consensus. *Mar Ecol Prog Ser*, 52, :77-88.
- Pope, R., et Fry E., 1997. Absorption spectrum (380-700 nm) of pure waters: II. Integrating cavity measurements. *Appl. Opt.*, 36, 8710-8723.
- Porter K.G. et Feig Y.S. 1980. The use of DAPI for identifying and counting aquatic microflora. *Limnol Oceanogr* 25, 943–948.
- Preisendorfer, R.W. 1961. Application of radiative transfer theory to light measurements in the sea. *Union Geod Geophys Inst Monogr* 10, Paris.
- Reynolds, R.A., Stramski, D. et Mitchell, B.G. 2001. A chlorophyll-dependent semianalytical reflectance model derived from field measurements of absorption and backscattering coefficients within the Southern Ocean. *J Geophys Res* 106(C4):7125-7138

- Roesler, C.S., et Boss, E. 2003. Spectral beam attenuation coefficient retrieved from ocean color inversion. *Geoph. Res. Lett.*, 30, 1468.
- Roman, M.R. 1984. Utilization of detritus by the copepod *Acartia tonsa*. *Limnol. Oceanogr.*, 29, 949-959.
- Romann, J., Valmalette, J.C., Røyset, A. et Einarsrud, M.A. 2015. Optical properties of single diatom frustules revealed by confocal microspectroscopy. *Opt. Lett.* 40, 740-743.
- Röttgers, R., Dupouy, C., Taylor, B. B., Bracher, A. et Woźniak, S. B.: Mass-specific light absorption coefficients of natural aquatic particles in the near-infrared spectral region, *Limnol. Oceanogr.*, 59, 1449–1460, 2014.
- Roy S., Blouin, F., Jacques, A. et Therriault, J.C. 2008. Absorption properties of phytoplankton in the lower estuary and Gulf of St Lawrence (Canada). *Can. J. of Fish. and Aquat. Sci.*, 65, 1721-1737.
- Sathyendranath, S. et Morel, A. 1983. Light emerging from the sea -interpretation and uses in remote sensing. In: Cracknell AP (ed) *Remote sensing applications in marine science and technology*. D Reidel Publishing Company. Dordrecht, p 323-357
- Sathyendranath, S., Prieur, L. et Morel, A. 1989. A three-component model of ocean colour and its application to remote sensing of phytoplankton pigments in coastal waters. *Int. J. Rem. Sens.*, 10, 1373-1394.
- Saucier, F. J., Roy, F., Senneville, S., Smith, G., Lefavre, D., Zakardjian, B. et Dumais, J.-F. 2009. Modelling of the circulation in the estuary and the Gulf of St. Lawrence in response to variations in fresh water runoff and winds. *Journal of Water Science*, 22: 159–176 (article in French).
- Schneider C.A., Rasband W.S. et Eliceiri K.W. 2012. NIH Image to ImageJ: 25 years of image analysis. *Nat Methods.*, 9, 671-675.
- Segschneider, J. et Bendtsen, J. 2013. Temperature-dependent remineralization in a warming ocean increases surface pCO₂ through changes in marine ecosystem composition. *Global Biogeochemical Cycles*, 27, 1214-1225.

- Sieracki, M. et Viles, C. 1992. Distributions and fluorochrome staining properties of sub-micrometer particles and bacteria in the North Atlantic. Deep-Sea Res. 39: 1919–1929.
- Sieracki, M.E., Johnson, P.W. et Sieburth, J.M. 1985. Detection, enumeration, and sizing of planktonic bacteria by image-analyzed epifluorescence microscopy. App. Environ. Microb., 49, 799-810.
- Smith, D.C. et Azam F. 1992. A simple, economical method for measuring bacterial protein synthesis rates in seawater using ^{3}H -leucine. Mar. Microb. Food Web, 6, 107–114.
- Snyder, W.A., Arnone, R.A., Davis, C.O., Goode, W., Gould, R.W., Ladner, S., Lamela, G., Rhea, W.J., Stavn, R., Sydor, M. et Weidemann, A. 2008. Optical scattering and backscattering by organic and inorganic particulates in U.S. coastal waters. Appl. Optics, 47, 666-677.
- Sosik, H.M. et Michell, G. 1995. Light absorption by phytoplankton, photosynthetic pigments and detritus in the California Current System. Deep-Sea Res., 42, 1717-1748.
- Stavn, R. H. et Richter, S.J. 2008. Biogeo-optics: Particle optical properties and the partitioning of the spectral scattering coefficient of ocean waters. Appl. Opt., 47, 2660–2679.
- Stavn, R.H., 2012. Mass-specific scattering cross sections of suspended sediments and aggregates: theoretical limits and applications. Opt. Express, 20, 201-219.
- Stramski, D., Boss, E., Bogucki, D. et Voss, K.J. 2004. The role of seawater constituents in light backscattering in the ocean. Progr. Oceanogr., 61, 27-56.
- Stramski, D., Bricaud, A. et Morel, A. 2001. Modeling the inherent optical properties of the ocean based on the detailed composition of the planktonic community. Appl. Opt., 40, 2929–2945.
- Stramski, D. et Kiefer, D. 1990. Optical properties of bacteria. SPIE Proc. 1302, Ocean Optics X, doi: 10.1117/12.21450.
- Stramski, D., et Kiefer, D.A. 1991. Light scattering by microorganisms in the open ocean. Prog. Oceanogr., 28, 343–383.

- Stramski, D. et Kiefer, D.A. 1998. Can heterotrophic bacteria be important to marine light absorption? *J. Plank. Res.*, 20, 1489-1500.
- Stramski, D. et Reynolds, R.A. 1993. Diel variations in the optical properties of a marine diatom. *Limnol. Oceanogr.*, 38, 1347-1364.
- Strickland, J.D.H. et Parsons, T.R. 1972. A practical handbook of seawater analysis. Bulletin (Fisheries Research Board of Canada), 167 (2nd ed.), Ottawa, Fisheries Research Board of Canada.
- Stukel M.R., 2014. Detritus in the pelagic ocean. Eco-DAS IX Symposium Proceedings, Association of Limnology and Oceanography, Chapter 3, 2014, 49-76.
- Sundby, B. 1974. Distribution and Transport of Suspended Particulate Matter in the Gulf of St. Lawrence. *Can. J. Earth Sci.*, 11, 1517-1533.
- Tassan, S. et Ferrari, G.M. 2002. A thorough sensitivity analysis of the ‘transmittance-reflectance’ method for measuring light absorption by aquatic particles. *J. Plank. Res.*, 24, 757-776.
- Thresher, R.E., Nichols, P.D., Gunn, J.S., Bruce, B.D. et Furlani, D.M. 1992. Seagrass detritus as the basis of a coastal food chain, *Limnol. Oceanogr.*, 37, 1754-1758.
- Tilstra, L.G. et Stammes, P. 2007. Earth reflectance and polarization intercomparison between SCIAMACHY onboard Envisat and POLDER onboard ADEOS-2. *J. Geoph. Res.*, 112, D11304, doi:10.1029/2006JD007713.
- Tomas, C.R. 1997. Identifying marine phytoplankton. Elsevier, Academic Press, p. 858, ISBN: 978-0-12-693018-4.
- Tremblay, L., Alaoui, G. et Leger, M.N. 2011. Characterization of Aquatic Particles by Direct FTIR Analysis of Filters and Quantification of Elemental and Molecular Compositions. *Environ. Sci. Tech.*, 45, 9671-9679.
- Turner, J.T. 2015. Zooplankton fecal pellets, marine snow, phytodetritus and the ocean’s biological pump. *Prog. Oceanogr.*, 130, 205-248.
- Turpie, K.R. 2013. Explaining the Spectral Red-Edge Features of Inundated Marsh Vegetation. *Journal of Coastal Research*, 290: 1111–1117. doi:10.2112/JCOASTRES-D-12-00209.1.

- Twardowski, M.S., Boss, E., Macdonald, J.B., Pegau, W.S., Barnard, A.H. et Zaneveld J.R.V. 2001. A model for estimating bulk refractive index from the optical backscattering ratio and the implications for understanding particle composition in case I and case II waters. *J. Geophys. Res.*, 106, C7, 14,129-14,142.
- Twardowski, M.S., Sullivan, J.M., Donaghay, P.L. et Zaneveld, J.R.V. 1999. Microscale quantification of the absorption by dissolved and particulate material in coastal waters with an ac-9. *J. Atm. and Ocean. Tech.*, 16, 691-707.
- Vaillancourt, R.D., Brown, C.W., Guillard, R.R., et Balch, W.M. 2004. Light backscattering properties of marine phytoplankton: relationships to cell size, chemical composition and taxonomy. *J. Plank. Res.*, 26, 191-212.
- Verity, P.G., Beatty, T.M., et Williams, S.C. 1996. Visualization and quantification of plankton and detritus using digital confocal microscopy. *Mar. Ecol. Progr. Ser.*, 10, 55-67.
- Verity, P.G., Williams, S.C., et Hong, Y. 2000. Formation, degradation, and mass:volume ratios of detritus derived from decaying phytoplankton. *Mar. Ecol. Progr. Ser.*, 207, 53-68.
- Vodacek, A. 1992. An explanation of the spectral variation in freshwater CDOM fluorescence. *Limnol Oceanogr* 37(8): 1808-1813.
- Vodacek, A., Blough, N.V., DeGrandpre, M.D., Peltzer, E.T. et Nelson, R.K. 1997. Seasonal variation of CDOM and DOC in the Middle Atlantic Bight: Terrestrial inputs and photooxidation. *Limnol. Oceanogr.*, 42(4):674-686.
- Vodacek, A., Hoge, F.E., Swift, R.N., Yungel, J.K., Peltzer, E.T. et Blough N.V. 1995. The use of in situ and airborne fluorescence measurements to determine UV absorption coefficients and DOC concentrations in surface waters. *Limnol. Oceanogr.*, 40, (2):411-415.
- Voss, K.J. 1992. A spectral model of the beam attenuation coefficient in the ocean and coastal areas. *Limnol. Oceanogr.*, 37, 501-509.
- Wei, J. et Lee, Z. 2015. Retrieval of phytoplankton and colored detrital matter absorption coefficients with remote sensing reflectance in an ultraviolet band. *Applied Optics*, 54, 636-649.

- Welschmeyer, N.A. 1994. Fluorometric analysis of chlorophyll a in the presence of chlorophyll b and pheopigments. Limnol. Oceanogr. 39, 1985-1992.
- Williams, S.C., Verity, P.G. et Beatty, T. 1995. A new staining technique for dual identification of plankton and detritus in seawater. J. Plank. Res., 17, 2037-2047.
- Woźniak B. et Pelevin V.N., 1991. Optical classifications of the seas in relation to phytoplankton characteristics Oceanologia, 31, 25-55.
- Wozniak, S.B., Meler, J., Lednika, B., Zdun, A. et Ston-Egiert, J. 2011. Inherent optical properties of suspended particulate matter in the Southern Baltic Sea. Oceanologia, 53, 691-729.
- Xie H., Aubry C., Bélanger S. et Song G, 2012. The dynamics of absorption coefficients of chromophoric dissolved organic matter and particles in the St. Lawrence estuarine system : Biogeochemical and physical implications. Marine Chemistry, 128-129, 44-56.
- Yamasaki, A., Fukuda, H., Fukuda, R., Miyakima, T., Nagata, T., Ogawa, H., et Koike, I. 1998. Submicrometer particles in northwest Pacific coastal environments: Abundance, size distribution, and biological origins. Limnol. Oceanogr. 43: 536–542.
- Yeats, P.A. 1988. Distribution and transport of suspended particulate matter. In: Strain, P.M. (Ed.), Chemical Oceanography in the Gulf of St. Lawrence. Dept. of Fisheries and Oceans, chapter 2, pp. 15-28, 1988.
- Yentsch, C.S. et Yentsch, C.M. 2008. Single cell analysis in biological oceanography and its evolutionary implications. J. Plankt. Res., 30, 107-117.
- Zaneveld, J.R.V., Kitchen, J.C., et Moore, C.M. 1994. The scattering correction error of the reflecting-tube absorption meters, Ocean Optics XII, J.S. Jaffe, Ed. International Society for Optical Engineering, SPIE proceedings, vol. 2258, 44-58.
- Zhang, X., Stavn, R. H., Falster, A. U., Gray, D., et Gould, R. W. 2014. New insight into particulate mineral and organic matter in coastal ocean waters through optical inversion, Estuar. Coast. Res. Shelf Sci., 149, 1–12.

Zhang, X., Twardowski, M., et Lewis, M. 2011. Retrieving composition and sizes of oceanic particle subpopulations from the volume scattering function. *Applied Optics*, 50, 1 240-1259.